J Nonlinear Sci
DOI 10.1007/s00332-012-9140-7

Journal of Nonlinear Science

Solving Optimal Control Problems by Exploiting Inherent Dynamical Systems Structures

Kathrin Flaßkamp · Sina Ober-Blöbaum · Marin Kobilarov

Received: 31 October 2011 / Accepted: 23 June 2012
© Springer Science+Business Media, LLC 2012

Abstract Computing globally efficient solutions is a major challenge in optimal control of nonlinear dynamical systems. This work proposes a method combining local optimization and motion planning techniques based on exploiting inherent dynamical systems structures, such as symmetries and invariant manifolds. Prior to the optimal control, the dynamical system is analyzed for structural properties that can be used to compute pieces of trajectories that are stored in a motion planning library. In the context of mechanical systems, these motion planning candidates, termed primitives, are given by relative equilibria induced by symmetries and motions on stable or unstable manifolds of e.g. fixed points in the natural dynamics. The existence of controlled relative equilibria is studied through Lagrangian mechanics and symmetry reduction techniques. The proposed framework can be used to solve boundary value problems by performing a search in the space of sequences of motion primitives connected using optimized maneuvers. The optimal sequence can be used as an admissible initial guess for a post-optimization. The approach is illustrated by two numerical examples,

Communicated by Oliver Junge.

K. Flaßkamp · S. Ober-Blöbaum (✉)
Computational Dynamics and Optimal Control, Department of Mathematics, University of Paderborn, Paderborn, Germany
e-mail: sinaob@math.upb.de

K. Flaßkamp
e-mail: kathrinf@math.upb.de

M. Kobilarov
Control and Dynamical Systems, California Institute of Technology, Pasadena, USA
e-mail: marin@cds.caltech.edu

Published online: 13 July 2012

the single and the double spherical pendula, which demonstrates its benefit compared to standard local optimization techniques.

Keywords Lagrangian mechanics · Optimal control · Symmetries · Invariant manifolds

Mathematics Subject Classification 37J15 · 49M37 · 70Q05

1 Introduction

This work combines classical methods from dynamical systems theory and recently developed numerical optimal control methods. The underlying motivation is to overcome one of the major limitations of current numerical control methods, namely the restriction to local optimality for optimal control solutions. The basic idea of the presented approach is to exploit the inherent dynamical properties of the system under consideration. These structures can be revealed by an analysis of the natural dynamics on the one hand, and the system's motion under the influence of specific controls on the other hand.

Optimal Control of Dynamical Systems Optimal control theory goes back to the work of Pontryagin on necessary optimality conditions in the last century, whereas its roots are attributed to Bernoulli because of his work on the brachistochrone problem dating from more than 300 years ago (Sussmann and Willems 1997). To this day, it is an important field of research, based on the question of how to force a system into a desired behavior in an optimal way. A typical problem formulation is as follows: which path of the system's dynamical states, forced by an admissible control trajectory, minimizes a given cost functional? Here, the space of all admissible state and control trajectories is infinite dimensional and additionally constrained by fixed boundary values and possibly further restrictions on the system's states or control input. Therefore, solving optimal control problems most often relies on numerical means. The developed methods can be divided into two classes (cf. Binder et al. 2001). Indirect methods apply the Pontryagin maximum principle to obtain a system of necessary optimality conditions and then solve these boundary value problems. In contrast, direct methods (cf. Betts 1998) begin with a discretization that transforms the optimal control problem to a nonlinear constrained optimization problem. Nonlinear programming methods, such as SQP (sequential quadratic programming, cf. e.g. Gill et al. 2000) can then be applied. However, typically, these are local solvers that cannot guarantee global optimality and require good initial guesses. A number of global optimization methods (e.g. Neumaier 2004; Zhigljavsky and Zilinskas 2008) have been developed to overcome these limitations.

This work develops a global approach that exploits special system structures related to dynamical symmetries. Preservation of such structures will also play a key role in the numerical approximation methods that we will develop. This is related to recent approaches in optimal control for mechanical systems that are structure preserving, i.e. the discretization preserves the system structures, e.g. symmetry or conserved quantities such as momenta, by using discrete variational mechanics (cf. Marsden and West 2001; Ober-Blöbaum et al. 2011). The structure exploiting

motion planning approach that we present provides state and control sequences that can serve as an admissible sophisticated initial guess to a post-optimization, e.g. by a local SQP method.

Applications of optimal control theory are numerous in many different areas of research. Optimal control methods have been successfully applied to electric power systems (Christensen et al. 1987) as well as to many different mechanical systems, e.g. in aerodynamics (Naldi and Marconi 2011) and space mission design (Dellnitz et al. 2009), in bio medicine, robotics (Leyendecker et al. 2009), and automotive engineering (Gerdts 2005).

Motion Planning In the last decades, there has been a growing importance of mechatronic systems as mechanical systems with embedded electronics and digital control units. This has led to multidisciplinary research on mechatronic systems as well, in particular regarding control issues. While classical control theory focuses on stability and feedback or on open loop control, the influence of planning methods from the field of artificial intelligence, i.e. discrete methods such as e.g. decision processes (cf. LaValle 2006) give rise to new kinds of motion planning approach that combine continuous and discrete methods. In this work, the term motion planning is used in the sense of generating open loop trajectories for dynamical systems. This will be accomplished by combining optimal control methods with discrete planning techniques based on search trees. Motion planning by *motion primitives* fits into this category of hybrid motion planning approaches. The idea is to solve the complex control problem by constructing a finite sequence of simple motion termed motion primitives. Frazzoli et al. (2005) explain that this approach can be deduced from the intuitive way in which human pilots steer helicopters, that is, by recurrent simple steering modes with short intermediate control maneuvers.

Following the idea of Frazzoli et al. (2005), we quantize the space of state and control trajectories by representative small pieces of solution curves which can be combined into various sequences. These motion primitives are stored in a *motion planning library*. The problem is thus reduced to searching for the optimal sequence out of all admissible sequences in the library which can be solved using global search methods. Problems with state constraints such as obstacles in the environment can be handled with the help of probabilistic roadmap methods (LaValle 2006; Choset et al. 2005). Candidates for the motion primitives can be obtained by the inherent dynamical properties of the system under consideration, such as motion along relative equilibria (cf. Sect. 3.2) or motions on stable or unstable manifolds of the natural dynamics (cf. Sect. 3.3).

Mechanical Systems and Symmetry The proposed motion planning approach is general and can be applied to arbitrary dynamical systems. However, we focus on optimal control of mechanical systems, because these systems exhibit well-studied structural properties (cf. e.g. Abraham and Marsden 1987; Marsden and Ratiu 1999; Bloch 2003; Bullo and Lewis 2004).

In geometric mechanics, mechanical systems are modeled by a variational approach. Hamilton's least action principle is based on the Lagrangian of the system and can be extended to systems underlying external forcing by the Lagrange–d'Alembert principle. This leads to the well known forced Euler–Lagrange equations as the sys-

tem's equations of motion. Variational mechanics can be directly discretized using discrete variations, e.g. for numerical simulation techniques or optimal control methods (e.g. Marsden and West 2001; Ober-Blöbaum et al. 2011). These so called geometric integrators are of great interest, because they preserve properties of the continuous system, such as symplecticity or conserved momenta induced by symmetry. In addition, they exhibit long-time stable energy behavior. An optimal control method for mechanical systems based on variational integrators is DMOC (*Discrete Mechanics and Optimal Control*, cf. (Ober-Blöbaum et al. 2011)) which will be described in Sect. 2.3.

In this work, we will study continuous symmetries that can be described by a Lie group action. For physical systems, this means the invariance of the Lagrangian with respect to translational or rotational motions. These properties are important in control, because a solution trajectory that has been designed for one specific situation, e.g. a turn maneuver for a helicopter, is suitable in many other cases as well, because it does not explicitly depend on the absolute position in space. More precisely, we will call two pairs of state and control trajectories of a symmetric system *equivalent*, if the states are related by a Lie group element and the pairs by a time shift, i.e. a spatiotemporal symmetry equivalence. Continuous symmetries in mechanical systems correspond to the conservation of momenta and to the existence of motions that are solely induced by symmetry, i.e. relative equilibria (cf. Sect. 3.2). For Hamiltonian and Lagrangian systems, relative equilibria can be determined analytically by symmetry reduction procedures (Marsden and Ratiu 1999; Marsden et al. 2000; Marsden 1993). Whereas relative equilibria and symmetry reduction for Hamiltonian systems have been comprehensively studied for several decades (see e.g. the textbooks of Marsden and Ratiu 1999; Marsden 1993 and for more recent work, e.g. Bullo and Lewis 2007; Roberts et al. 2002), reduction procedures directly on Lagrangian systems have gained less attention (cf. Marsden and Scheurle 1993). Related work studies symmetry properties of relative equilibria and design feedback control laws directly based on a symmetry splitting of the state space (Simo et al. 1991; Bloch et al. 2000). Families of relative equilibria in Hamiltonian systems can be numerically computed by path following methods to study e.g. bifurcation phenomena (Wulff and Schilder 2009).

There also exists an intensive research in mechanical (control) systems on Lie groups, i.e. if the overall state space has Lie group structure (see e.g. Bullo and Lewis 2004 or Kobilarov and Marsden 2011). To avoid confusion, in our setting the configuration manifold is an arbitrary manifold Q on which a Lie group G operates by symmetry actions $\Phi : G \times Q \to Q$. Typically the invariance is found only in some coordinates, thus the remaining coordinates have to be left unchanged by the symmetry action. If the Lagrangian of a mechanical system does not explicitly depend on a coordinate (but on the corresponding velocities), it is called *cyclic*. Reduction of cyclic Lagrangian was considered by Routh (see e.g. Marsden and Ratiu 1999), who called relative equilibria *steady motions* since they are the equilibrium points of the reduced Euler–Lagrange equations. In Sect. 5.1 the simple spherical pendulum is considered as an example of a cyclic Lagrangian system. In contrast, the double spherical pendulum is not cyclic and therefore has to be addressed by the extended *Lagrangian reduction* (see Marsden and Scheurle 1993 and Sects. 3.2 and 5.2).

Invariant Manifolds in Natural Dynamics In the control of mechanical, electrical or mechatronic systems, minimizing the energetic effort is often of particular importance. Thus it is obvious that trajectories of the natural, i.e. uncontrolled dynamics that are free of cost, should be used whenever the planning scenario allows for it. However, even the natural dynamics of nonlinear systems are typically quite complicated such that an analysis, by analytical and / or numerical means, is necessary to identify promising candidates for planning scenarios. In this work, we study the use of trajectories on (un)stable manifolds of the natural dynamics for motion planning purposes. The manifolds arise at invariant objects, in the simplest case an equilibrium or a periodic orbit. Near these critical objects, the manifolds are tangent to the eigenspaces of the system's linearization. Eigenvalues with zero real part give rise to so called center manifolds. Conversely, if the spectrum is hyperbolic, i.e. it has no eigenvalues on the imaginary axis, the stable and unstable invariant subspaces span the entire state space. The stable manifold consists of all points that tend to the critical object under the system's flow; points of the unstable manifold show the same behavior in backward time (see any textbook on dynamical systems, e.g. Guckenheimer and Holmes 1983 or Abraham and Marsden 1987 for a focus on Hamiltonian and Lagrangian systems). We will go into this in more detail in Sect. 3.3.

Since the studies of orbit structures in celestial mechanics performed in Conley (1968), McGehee (1969), invariant manifolds have been exploited in this spirit for a variety of space mission trajectories for the energy efficient transport between different planets and their nearby orbits (see e.g. Gómez et al. 2004; Koon et al. 2001 among numerous others). This concept has been extended in such a way that (un)stable manifolds of several different systems are used as partial orbits that are concatenated by appropriately controlled maneuvers (see e.g. Koon et al. 2000 and related work of these authors or Dellnitz et al. 2009).

Throughout the present work, all (uncontrolled) systems are assumed to be autonomous, i.e. not explicitly time-dependent except for the control force that is a function of time. However, in a non-autonomous setting, which arises e.g. when studying fluid dynamics or ocean flow dynamics, organizing structures that are related to (un)stable manifolds, e.g. Lagrangian coherent structures, have been detected (Haller 2001; Haller and Yuan 2000) and studied in a number of preceding works (see e.g. Froyland and Padberg 2009 for a comparing description of computational techniques).

Contributions This work extends recent results on motion planning for systems with symmetries (Frazzoli et al. 2005) to include new kinds of motion primitive—trajectories along stable or unstable manifolds of equilibria or periodic orbits. Thus, the resulting solutions exploit the structure of the system dynamics to a higher degree. On the theoretical side, the study of relative equilibria in geometric mechanics is extended to mechanical systems with a special kind of control forces. This enables us to identify candidates that satisfy the definition of trim primitives. In addition, maneuvers which serve as transition in the motion library are designed using structure-respecting optimal control that provably preserves symmetries and motion invariants. We develop a numerical framework based on (un)stable manifolds, relative equilibria, and optimized maneuvers and apply it to a nontrivial example, the double spherical pendulum.

The outline is as follows: In Sect. 2 a short introduction in optimal control formulations, variational mechanics and the optimal control method DMOC is given. Next, we analyze the inherent dynamical structures of mechanical systems that can be exploited for optimal control in Sect. 3, i.e. symmetry, relative equilibria and (un)stable manifolds. In Sect. 4 it is explained in detail, how we perform the motion planning with primitives. Numerical results for two examples, a simple and a double spherical pendulum are presented in Sect. 5 which have been partly presented in a short version of this work in Flaßkamp and Ober-Blöbaum (2012). Finally, Sect. 6 concludes by pointing out several directions of further research.

2 Preliminaries

In this work, optimal control problems for complex nonlinear systems are studied and solved by numerical methods. Here, we focus on systems that can be modeled by Lagrangian mechanics. In this section, we briefly introduce the framework our research is based upon.

2.1 Optimal Control

Consider a system with time-dependent state $x(t) \in X$ controlled using time-dependent actuator input $u(t) \in U$, where X is the state space and U denotes the set of controls. The dynamics is described by the function $f : X \times U \to TX$ defined by

$$\dot{x}(t) = f\big(x(t), u(t)\big), \tag{1}$$

which is used to evolve the state forward in time. In addition, the system is subject to constraints arising from actuator bounds and forbidden regions in the state space. These constraints are expressed through the vector of inequalities

$$h\big(x(t), u(t)\big) \geq 0, \tag{2}$$

for all $t \in [0, t_\mathrm{f}]$, where $t_\mathrm{f} > 0$ is the final time of the trajectory. The goal is to compute the optimal controls u^* and time t_f^* driving the system from its initial state $x_0 \in X$ to a given goal region $\mathcal{X}_\mathrm{f} \subset X$, i.e.

$$\begin{aligned} \big(u^*, t_\mathrm{f}^*\big) &= \arg\min_{u, t_\mathrm{f}} \int_0^{t_\mathrm{f}} C\big(x(t), u(t)\big)\,\mathrm{d}t, \\ \text{subject to} \quad & \dot{x}(t) = f\big(x(t), u(t)\big), \\ & h\big(x(t), u(t)\big) \geq 0, \quad x(0) = x_0,\ x(t_\mathrm{f}) \in \mathcal{X}_\mathrm{f} \end{aligned} \tag{3}$$

for all $t \in [0, t_\mathrm{f}]$ and where $C : X \times U \to \mathbb{R}$ is a given cost function. A typical cost function includes a time component and a control effort component, e.g. $C(x(t), u(t)) = \lambda_1 \cdot 1 + \lambda_2 \cdot \|u(t)\|^2$ where $\lambda_{1,2} \geq 0$ are chosen weights and $\|\cdot\|$ is the 2-norm. The problem (3) has no closed-form solution since both the dynamics (1) and constraints (2) are nonlinear.

There exist a number of different approaches for numerically solving optimal control problems, for a good overview we recommend Binder et al. (2001) and the references therein. The solution methods can be divided into indirect and direct methods. While indirect methods generate and then solve a boundary value problem according to the necessary optimality conditions of the Pontryagin maximum principle (cf. e.g. Binder et al. 2001), direct methods start with a discretization of the problem (3). Thus one obtains a nonlinear optimization problem that can be addressed by appropriate state of the art techniques such as sequential quadratic programming (SQP, cf. e.g. Gill et al. 2000). These methods require derivative information of the constraints and the objective, which can be either approximated by finite differences, or provided by analytical expressions if at hand, or computed by algorithmic differentiation (cf. Griewank and Walther 2008).

However, gradient-based optimization is not suitable unless a good starting guess is chosen since typically there are many local minima. Thus, instead of solving (3) numerically using a black box nonlinear programming tool such as SQP we reformulate the problem by exploiting any existing structure in the dynamics. This is accomplished by considering symmetries and invariant manifolds described in Sect. 3.

2.2 Variational Mechanics

An important class of dynamical systems that are rich in inherent structural properties are mechanical systems. The study of mechanical systems from the perspective of differential geometry has a long history (cf. e.g. Abraham and Marsden 1987; Marsden and Ratiu 1999; Marsden and West 2001). However, geometric mechanics is an active field of research, in particular regarding optimal control problems (Bloch 2003; Bullo and Lewis 2004; Ober-Blöbaum et al. 2011). The following descriptions are mainly taken from Flaßkamp and Ober-Blöbaum (2012).

Let Q be an n-dimensional configuration manifold with tangent bundle TQ and cotangent bundle T^*Q. Consider a mechanical system with time-dependent configuration vector $q(t) \in Q$ and velocity vector $\dot{q}(t) \in T_{q(t)}Q$, $t \in [0, t_\mathrm{f}]$, whose dynamical behavior is described by the Lagrangian $L : TQ \to \mathbb{R}$. Typically, the Lagrangian L consists of the difference of the kinetic and potential energy. In addition, there is a force $f : TQ \times U \to T^*Q$ acting on the system. This force depends on a time-dependent control parameter $u(t) \in U \subseteq \mathbb{R}^m$ that influences the system's motion. The equations of motion can be described via a variational principle. Define the *action map* $\mathfrak{S} : C^2([0, t_\mathrm{f}], Q) \to \mathbb{R}$ as

$$\mathfrak{S}(q) = \int_0^{t_\mathrm{f}} L\big(q(t), \dot{q}(t)\big)\,\mathrm{d}t.$$

Then the *Lagrange–d'Alembert principle* seeks curves $q \in C^2([0, t_\mathrm{f}], Q)$ with fixed initial value $q(0)$ and fixed final value $q(t_\mathrm{f})$ satisfying

$$\delta \int_0^{t_\mathrm{f}} L(q, \dot{q})\,\mathrm{d}t + \int_0^{t_\mathrm{f}} f(q, \dot{q}, u) \cdot \delta q\,\mathrm{d}t = 0 \tag{4}$$

for all variations $\delta q \in T_q C^2([0, t_\mathrm{f}], Q)$, where the second integral in (4) is the *virtual work* acting on the mechanical system via the force f. This yields the *forced Euler–Lagrange equations*

$$\frac{\partial L}{\partial q}(q, \dot{q}) - \frac{\mathrm{d}}{\mathrm{d}t}\left(\frac{\partial L}{\partial \dot{q}}(q, \dot{q})\right) + f(q, \dot{q}, u) = 0. \tag{5}$$

For the unforced Euler–Lagrange equations ($f = 0$), we denote the *Lagrangian vector field* by X_L and by $F_\mathrm{L} : TQ \times [0, t_\mathrm{f}] \to TQ$ its *flow*. If we fix the time t, we write $F_\mathrm{L}^t : TQ \to TQ$. In case there is external forcing acting on the system, (5) implicitly defines a family of *forced Lagrangian flows* F_L^u for fixed curves $u : [0, t_\mathrm{f}] \to U$. The *forced Lagrangian vector field* is then denoted by X_L^u.

2.3 Discrete Mechanics and Optimal Control

To formulate the optimal control problem for controlled Lagrangian systems, we replace in Sect. 2.1 the state space X by the tangent bundle TQ by setting $x(t) = (q(t), \dot{q}(t))$ and replace the differential equation in the optimal control problem (3) by the forced Euler–Lagrange equations (5). Recently, the direct optimal control method DMOC (*Discrete Mechanics and Optimal Control*, Ober-Blöbaum et al. 2011) was developed to numerically solve optimal control problems of Lagrangian systems and thereby taking the special structure of mechanical systems into account. Using concepts from discrete variational mechanics, DMOC is based on a direct discretization of the Lagrange–d'Alembert principle of the mechanical system. The goal of discrete variational mechanics is to derive discrete approximations of the solutions of the forced Euler–Lagrange equations that inherit the same qualitative behavior as the continuous solution.

The continuous optimal control problem is transformed into a finite dimensional constrained optimization problem using a global discretization of the states and the controls. The state space TQ is replaced by $Q \times Q$ and the discretization grid is defined by $\Delta t = \{t_k = kh \mid k = 0, \ldots, N\}$, $Nh = t_\mathrm{f}$, where N is a positive integer and h is the step size. The path $q : [0, t_\mathrm{f}] \to Q$ is replaced by a discrete path $q_\mathrm{d} : \{t_k\}_{k=0}^N \to Q$, where $q_k = q_\mathrm{d}(kh)$ is an approximation to $q(kh)$ (Marsden and West 2001; Ober-Blöbaum et al. 2011). Similarly, the control path $u : [0, t_\mathrm{f}] \to U$ is replaced by a discrete one. To this end, a refined grid, $\Delta\tilde{t}$, is generated via a set of control points $0 \le c_1 < \cdots < c_s \le 1$ and $\Delta\tilde{t} = \{t_{k\ell} = t_k + c_\ell h \mid k = 0, \ldots, N-1; \ell = 1, \ldots, s\}$. The discrete control path is defined to be $u_\mathrm{d} : \Delta\tilde{t} \to U$. The intermediate control samples $u_k = (u_{k1}, \ldots, u_{ks}) \in U^s$ on $[t_k, t_{k+1}]$ are defined to be the values of the control parameters guiding the system from $q_k = q_\mathrm{d}(t_k)$ to $q_{k+1} = q_\mathrm{d}(t_{k+1})$, where $u_{kl} = u_\mathrm{d}(t_{kl})$ for $l \in \{1, \ldots, s\}$.

To construct a discrete version of the Lagrange–d'Alembert principle, a *discrete Lagrangian* $L_\mathrm{d} : Q \times Q \to \mathbb{R}$ is defined that approximates the action integral along the curve segment between two adjacent points q_k and q_{k+1} as

$$L_\mathrm{d}(q_k, q_{k+1}) \approx \int_{kh}^{(k+1)h} L\big(q(t), \dot{q}(t)\big)\,\mathrm{d}t. \tag{6}$$

The *discrete action* is given by the sum of the discrete Lagrangian on each adjacent pair $\mathfrak{S}_\mathrm{d}(q_\mathrm{d}) = \sum_{k=0}^{N-1} L_\mathrm{d}(q_k, q_{k+1})$. Similarly, the virtual work can be approximated via

$$\sum_{k=0}^{N-1} f_\mathrm{d}^-(q_k, q_{k+1}, u_k) \cdot \delta q_k + f_\mathrm{d}^+(q_k, q_{k+1}, u_k) \cdot \delta q_{k+1} \approx \int_0^{t_\mathrm{f}} f\big(q(t), \dot{q}(t), u(t)\big) \cdot \delta q(t)\,\mathrm{d}t \tag{7}$$

with the left and right discrete forces $f_\mathrm{d}^\pm(q_k, q_{k+1}, u_k) := f_k^\pm$. Based on these discrete objects, the *discrete Lagrange–d'Alembert principle* seeks discrete curves of points $\{q_k\}_{k=0}^N$ satisfying

$$\delta\mathfrak{S}_\mathrm{d} + \sum_{k=0}^{N-1} f_k^- \cdot \delta q_k + f_k^+ \cdot \delta q_{k+1} = 0 \tag{8}$$

for all variations δq_k vanishing at the endpoints. With $\delta q_0 = \delta q_N = 0$, (8) is equivalent to the *discrete forced Euler–Lagrange equations*

$$D_1 L_\mathrm{d}(q_k, q_{k+1}) + D_2 L_\mathrm{d}(q_{k-1}, q_k) + f_k^- + f_{k-1}^+ = 0 \tag{9}$$

for each $k = 1, \ldots, N-1$, where D_i denotes the derivative w.r.t. the ith argument. For given control values u_k, (9) provides a time stepping scheme for the simulation of the mechanical system which is called a *variational integrator* (cf. Marsden and West 2001). Since these integrators, derived in a variational way, are structure preserving, important properties of the continuous system are preserved (or change consistently with the applied forces), such as symplecticity or momentum maps induced by symmetries. In addition, they have an excellent long-time energy behavior. However, rather than solving initial value problems, an optimal control problem has to be solved, which involves the minimization of a cost functional $J(x,u) = \int_0^{t_\mathrm{f}} C(x(t), u(t))\,\mathrm{d}t$. Thus, in the same manner, an approximation of the cost functional generates the discrete cost functions C_d and J_d, respectively. The resulting nonlinear restricted optimization problem reads

$$\min_{q_\mathrm{d}, u_\mathrm{d}} J_\mathrm{d}(q_\mathrm{d}, u_\mathrm{d}) = \min_{q_\mathrm{d}, u_\mathrm{d}} \sum_{k=0}^{N-1} C_\mathrm{d}(q_k, q_{k+1}, u_k) \tag{10}$$

subject to the discrete forced Euler–Lagrange equations (9) and optionally discretized boundary and (in-)equality constraints for states and / or controls. Thus, the discrete forced Euler–Lagrange equations serve as equality constraints for the optimization problem which can be solved by standard optimization methods like SQP.

The approximation order of the optimal control scheme depends on the quadrature rule used to approximate the relevant integrals in (6) and (7). In general, one uses polynomial approximations to the trajectories and numerical quadrature to approximate the integrals. Then the order of the discrete Lagrangian and the discrete

forces is given by the order of the quadrature rule in use (e.g. second order using a midpoint rule approximation and assuming constant control parameters on each time interval with $l = 1$ and $c_1 = \frac{1}{2}$).

In Ober-Blöbaum et al. (2011), a detailed analysis of DMOC resulting from this discrete variational approach is given. The optimization scheme is symplectic-momentum consistent, i.e. the symplectic structure and the momentum maps corresponding to symmetry groups are consistent with the control forces for the discrete solution independent on the step size h. Thus, the use of DMOC leads to a reasonable approximation to the continuous solution, also for large step sizes, i.e. a small number of discretization points. In this work, DMOC will be used to compute the short controlled maneuvers mentioned above as well for a post-optimization of the found sequence. DMOC maneuvers combined with trims have been successfully used before in Kobilarov (2008) to build up a motion planning library for the optimal control of an autonomous helicopter.

3 Structures in Mechanical Systems

The structure of mechanical systems is now studied in more detail. Each of the listed properties below can be advantageously used in the motion planning approach for optimal control problems. While symmetry exploiting methods in motion planning using trim primitives has been already proposed in Frazzoli et al. (2005), the incorporation of trajectories on (un)stable manifolds in this framework came up quite recently (Flaßkamp et al. 2010; Flaßkamp and Ober-Blöbaum 2012), motivated by successful applications of (un)stable manifolds in space mission design (e.g. Serban et al. 2002).

3.1 Symmetry

Symmetries are present in a variety of mechanical systems and have been extensively studied and analyzed during the last years. In this section the general setting of symmetries in mechanical systems is introduced. We mainly follow the concept of Marsden and West (2001). For a detailed formulation and analysis of symmetries in unforced Lagrangian systems we also refer to Marsden (1994), Marsden and Ratiu (1999), Bloch (2003), Marsden and Scheurle (1993).

Assume a *Lie group* G with Lie algebra $\mathfrak{g}$ acts on the configuration manifold Q by a *left-action* $\Phi : G \times Q \to Q$. For each $g \in G$ we denote by $\Phi_g : Q \to Q$ the diffeomorphism defined by $\Phi_g := \Phi(g, \cdot)$. Let $\Phi^{TQ} : G \times TQ \to TQ$ for $(q, v) \in TQ$ be the tangent lift of the action given by $\Phi_g^{TQ}(q, v) = T(\Phi_g) \cdot (q, v)$. The symmetry of the unforced mechanical system corresponds to the invariance of the Lagrangian under the group action, i.e. $L \circ \Phi_g^{TQ} = L$ for all $g \in G$. One also says: the group action is a symmetry of the Lagrangian. The presence of a symmetry leads to the notion of equivalent trajectories in the following way.

Definition 3.1 (Equivalence of trajectories) Two trajectories $\pi_1 : t \in [t_{\mathrm{i},1}, t_{\mathrm{f},1}] \mapsto (q_1(t), \dot{q}_1(t), u_1(t))$ and $\pi_2 : t \in [t_{\mathrm{i},2}, t_{\mathrm{f},2}] \mapsto (q_2(t), \dot{q}_2(t), u_2(t))$ of (5) are equivalent, if we have

(i) $t_{\mathrm{f},1} - t_{\mathrm{i},1} = t_{\mathrm{f},2} - t_{\mathrm{i},2}$ and
(ii) there exist a $g \in G$ and a $T \in \mathbb{R}$, such that $(q_1, \dot{q}_1)(t) = \Phi_g^{TQ}((q_2, \dot{q}_2)(t - T))$ and $u_1(t) = u_2(t - T)$ $\forall t \in [t_{\mathrm{i},1}, t_{\mathrm{f},1}]$.

Thus, equivalent trajectories can be constructed by a group action and a time shift only. All equivalent trajectories can be summed up in an equivalent class. By a slight abuse of notation, we call the equivalent class, but also its representative, a *motion primitive* (cf. Frazzoli et al. 2005). The number of candidates for the motion planning library can be immensely reduced by exploiting the system's invariance. Only one representative has to be stored and can then be used in different regions of the state space by a transformation of the lifted action.

Invariance and Lagrangian Flows Since G leaves the set of solutions of the variational principle invariant, the group action commutes with the Lagrangian flow F_{L} (Marsden et al. 1998). Furthermore, the invariance of the Lagrangian leads to the preservation of specific quantities by the Lagrangian flow.

For $\xi \in \mathfrak{g}$, let $\Phi^{\xi} : \mathbb{R} \times Q \to Q$ be the $\mathbb{R}$-action given by $\Phi^{\xi}(t, q) = \Phi(\exp(t\xi), q)$. The *infinitesimal generator* defined as $\xi_Q(q) = \frac{\mathrm{d}}{\mathrm{d}t}|_{t=0} \Phi(\exp(t\xi), q)$ is a vector field on Q while $\Phi(\exp(t\xi), \cdot) : Q \to Q$ is the corresponding flow on Q.

Assume that $L(q, v) = T(q, v) - V(q)$, where $V(q)$ is a G-invariant potential. G acts by isometries on the kinetic energy term, which can be written as $T(q, v) = \frac{1}{2} v^{\mathrm{T}} M(q) v = \frac{1}{2} \langle\langle v, v \rangle\rangle$ with mass matrix M and $\langle\langle \cdot, \cdot \rangle\rangle$ its induced inner product. The *Lagrangian momentum map* for a G-invariant Lagrangian L is defined by $\langle J(q, v), \xi \rangle = \langle \frac{\partial L}{\partial \dot{q}}(q, v), \xi_Q(q) \rangle = \langle\langle v, \xi_Q(q) \rangle\rangle$. Here, $\langle \cdot, \cdot \rangle$ denotes the natural pairing between elements of $T_q Q$ and its dual $T_q^* Q$.

The symmetry of Lagrangian systems leads to preservation of the associated momentum map as stated by Noether's theorem (see e.g. Marsden and West 2001).

Theorem 3.2 (Noether's Theorem) *Let $L : TQ \to \mathbb{R}$ be invariant under the lift of the action $\Phi : G \times Q \to Q$ as defined above, then the corresponding Lagrangian momentum map $J : TQ \to \mathfrak{g}^*$ is a conserved quantity for the flow, i.e. $J \circ F_{\mathrm{L}}^t = J$ for all times t.*

In general, arbitrary forcing would destroy the symmetry of Lagrangian systems since it breaks the conservation of the momentum map. However, as the forced Noether's theorem states, forcing that is orthogonal to the group action preserves symmetry (Marsden and West 2001; Ober-Blöbaum et al. 2011).

Theorem 3.3 (Forced Noether's Theorem) *Let the Lagrangian L and the symmetry action Φ be as in Theorem 3.2. Consider a force $f_{\mathrm{L}} : TQ \times U \to T^*Q$ such that $\langle f_{\mathrm{L}}(q, \dot{q}, u), \xi_Q(q) \rangle = 0$ for all $(q, \dot{q}) \in TQ$, $u(t) \in U$ $\forall t$ and all $\xi \in \mathfrak{g}$. Then the Lagrangian momentum map $J : TQ \to \mathfrak{g}^*$ is preserved by the forced Lagrangian flow, i.e. $J \circ (F_{\mathrm{L}}^u)^t = J$ for all t.*

3.2 Relative Equilibria and Trim Primitives

The presence of symmetry gives rise to the existence of a special kind of trajectories, i.e. motions that are solely generated by the symmetry action. These group orbits are therefore called *relative equilibria*.

Definition 3.4 (Relative equilibrium) A point $x_e = (q_e, v_e) \in TQ$ is called a relative equilibrium, if $X_L(x_e) \in T_{x_e}(G \cdot x_e)$, i.e. the Lagrangian vector field X_L at x_e points in the direction of the group orbit $G \cdot x_e = \{x = (q, v) | (q, v) = \Phi_g^{TQ}(q_e, v_e) \text{ for } g \in G\}$.

Finding relative equilibria is closely related to reduction processes, since relative equilibria correspond to fixed points of reduced equations of motion (Marsden 1993). Roughly speaking, the conservation of momentum maps (as stated by Noether's theorem) can be used to reduce the system's dynamic equations by constraining them to a fixed momentum value. In the following we give a brief overview of Lagrangian reduction techniques.

Lagrangian Reduction The symmetry reduction method for Lagrangian systems is called the *Lagrangian reduction method* and can be seen as the counterpart of the common *symplectic reduction method* or *energy-momentum method* for Hamiltonian systems. Lagrangian reduction (cf. Marsden and Scheurle 1993) is a generalization of the classical Routh reduction (see e.g. Bloch 2003) for cyclic variables. In the following, we recall some results of Marsden and Scheurle (1993) that equip us with a method to compute relative equilibria for mechanical systems and that can be extended to Lagrangian systems with forcing.

For each $q \in Q$ the *locked inertia tensor* $\mathbb{I} : \mathfrak{g} \to \mathfrak{g}^*$ is defined by $\langle \mathbb{I}(q)\eta, \zeta \rangle = \langle\langle \eta_Q(q), \zeta_Q(q) \rangle\rangle$ with η_Q, ζ_Q being the infinitesimal generators to $\eta, \zeta \in \mathfrak{g}$. It can be interpreted as the inertia tensor of a system which moves only in the direction of the infinitesimal generators of the symmetry action, as e.g. a multi-body system that has been locked to a rigid structure. The corresponding angular velocity is then given by $\alpha(q, v) = \mathbb{I}(q)^{-1} J(q, v)$, called the *mechanical connection*. For each $\mu \in \mathfrak{g}^*$, it leads to the definition of a one form on Q, denoted by α_μ with $\langle \alpha_\mu(q), v \rangle = \langle \mu, \alpha(q, v) \rangle$. The *amended potential* is defined by $V_\mu(q) = V(q) + \frac{1}{2}\langle \mu, \mathbb{I}(q)^{-1}\mu \rangle$ (cf. Marsden and Scheurle 1993) and plays an important role in reduction processes. For a given value $\mu \in \mathfrak{g}^*$ of the momentum map, the Routhian $R^\mu : TQ \to \mathbb{R}$ is defined as $R^\mu(q, v) = L(q, v) - \langle \alpha(q, v), \mu \rangle$. Fixing the level set of the momentum map, i.e. $J(q, \dot{q}) = \mu$ it can be shown (see Marsden and Scheurle 1993 for the variational derivation) that the original Euler–Lagrange equations are equivalent to the Euler–Lagrange equations of the Routhian R^μ with an additional gyroscopic forcing term, reading

$$\frac{\mathrm{d}}{\mathrm{d}t}\frac{\partial R^\mu}{\partial \dot{q}} - \frac{\partial R^\mu}{\partial q} = \dot{q}^{\mathrm{T}} \beta.$$

Here, β is the *magnetic two form* on Q, $\beta(q) : T_qQ \times T_qQ \to \mathbb{R}$, defined by $\beta = \mathbf{d}\alpha_\mu$, i.e. in coordinates, $\beta_{ij} = \frac{\partial \alpha_j}{\partial q^i} - \frac{\partial \alpha_i}{\partial q^j}$. (Recall that α_μ is a one form on Q, so in coordinates, $\alpha_\mu = \alpha_i \, \mathrm{d}q^i$ with $\mathrm{d}q^i$ being the basis vectors for T_q^*Q.) Based on

a splitting of the configuration manifold into the symmetry group G and the shape space $S = Q/G$, each vector $(q, v) \in T_q Q$ can be decomposed into its horizontal and its vertical part, $v = \mathrm{hor}_q v + \mathrm{ver}_q v$, where $\mathrm{ver}_q v = [\alpha(q, v)]_Q(q)$ and $\mathrm{hor}_q v = v - \mathrm{ver}_q v$. That means, the vertical part belongs to the vertical space of the connection and consists of all points that are mapped to zero under the projection from Q to S. These are the infinitesimal generators. The horizontal part is an element of the space that is orthogonal to the G-orbits, given by $\mathrm{hor}_q = \{(q, v) | J(q, v) = 0\}$. In Marsden and Scheurle (1993), it is shown that for fixed level sets of J, the Routhian can be reduced to $R^\mu = \frac{1}{2}\|\mathrm{hor}(q, v)\|^2 - V_\mu$. Hence, the Euler–Lagrange equations for R^μ can be reduced as well and the following statement can be deduced (cf. e.g. Marsden and Scheurle 1993, Prop. 3.5):

Proposition 3.5 *A point $x_\mathrm{e} = (q_\mathrm{e}, v_\mathrm{e})$ is a relative equilibrium if and only if q_e is a critical point of the amended potential V_μ with $\mu = J(q_\mathrm{e}, v_\mathrm{e})$.*

For control purposes it makes sense to generalize the definition of relative equilibria to forced systems by allowing constant control values. We will use the terminology of Frazzoli et al. (2005) and call them *trim primitives* originated from *trimmed motions*.

Definition 3.6 (Trim primitives) A point $x_\mathrm{e} = (q_\mathrm{e}, v_\mathrm{e})$ together with some control value $u_\mathrm{e} \in U$ is called a *trim primitive* (or shortly a *trim*), if we have $X_\mathrm{L}^{u_\mathrm{e}}(x_\mathrm{e}) \in T_{x_\mathrm{e}}(G \cdot x_\mathrm{e})$ with the forced Lagrangian vector field $X_\mathrm{L}^{u_\mathrm{e}}$.

In other words, trims generate solutions $(q(t), \dot{q}(t))$ on $[0, t_\mathrm{f}]$ of the forced Euler–Lagrange equations with control $u(t)$ for a G-invariant Lagrangian L and forcing f_L, which can be written as $(q, \dot{q})(t) = \Phi^{TQ}(\exp(t\xi), (q_\mathrm{e}, v_\mathrm{e}))$, $u(t) = u_\mathrm{e} = \text{const.}$ $\forall t \in [0, t_\mathrm{f}]$ with $\xi \in \mathfrak{g}$ and $\exp : \mathfrak{g} \to G, \xi \mapsto \exp(t\xi) \in G$. Trims are uniquely defined by their initial value $(q_0, \dot{q}_0, u_0)$ and the Lie algebra element ξ, which makes them easy to store and handle in a library of motion primitives. A second benefit of trims is that they are simply parametrized by time, i.e. their duration need not be fixed in advance, but can be adjusted during the sequencing (cf. Frazzoli et al. 2005).

In the following we will introduce the concept of controlled potentials that provides a method to construct trim primitives based on the computation of relative equilibria.

Controlled Potentials We augment the original potential $V(q)$ by a parameter-dependent term, representing potential forces, i.e. a special kind of forcing that is defined by a potential (cf. Bullo and Lewis 2004). That means, we replace $V : Q \to \mathbb{R}$ by $V^u : Q \to \mathbb{R}$, $V^u(q) = V(q) - v(q)$ with $v : Q \to \mathbb{R}$ having the property that $\frac{\partial}{\partial q} v(q) = u$ for some control value $u \in U$, where we assume that $U \subseteq \mathbb{R}^n$.

This type of control is intrinsically restricted to depend on configurations, so cannot be used to model dissipative, i.e. velocity dependent forces. However, many examples of control forces on mechanical systems fit into this structure.

The following theorem describes how a trim primitive for a controlled Lagrangian system can be computed by means of the concept of controlled potentials.

Theorem 3.7 *Let $L = T - V$ be a G-invariant Lagrangian and $V^u(q) = V(q) - v(q)$ the augmented, G-invariant controlled potential. The critical points of the amended controlled potential V^u_μ are relative equilibria of the forced Lagrangian vector field, X^u_{L}, i.e. trim primitives according to Definition 3.6.*

Proof Amending the controlled potential V^u leads to the amended controlled potential $V^u_\mu = V^u + \frac{1}{2}\langle \mu, \mathbb{I}(q)^{-1}\mu\rangle = V(q) - v(q) + \frac{1}{2}\langle \mu, \mathbb{I}(q)^{-1}\mu\rangle = V_\mu - v(q)$. Since we assume V^u to be G-invariant, Proposition 3.5 can be applied to the modified system given by the Lagrangian $L^u = T - V^u$, i.e. relative equilibria are given by the critical points of V^u_μ:

$$\frac{\partial}{\partial q} V^u_\mu = 0 \quad \Leftrightarrow \quad \frac{\partial}{\partial q}\big(V_\mu - v(q)\big) = 0 \quad \Leftrightarrow \quad \frac{\partial}{\partial q} V_\mu = u.$$

In other words, if a pair $(x_{\mathrm{e}}, u_{\mathrm{e}}) = ((q_{\mathrm{e}}, v_{\mathrm{e}}), u_{\mathrm{e}})$ satisfies $\frac{\partial}{\partial q} V_\mu(q_{\mathrm{e}}) = u_{\mathrm{e}}$ with $\mu = J(q_{\mathrm{e}}, v_{\mathrm{e}})$, the definition of a relative equilibrium, $X_{L^u}(x_{\mathrm{e}}) \in T_{x_{\mathrm{e}}}(G \cdot x_{\mathrm{e}})$, is fulfilled. The Euler–Lagrange equations of L^u read as follows: $\frac{\partial}{\partial q}(T(q,\dot q) - V^u(q)) - \frac{\mathrm{d}}{\mathrm{d}t}\frac{\partial}{\partial \dot q} T(q,\dot q) = \frac{\partial}{\partial q}(T(q,\dot q) - V(q)) - \frac{\mathrm{d}}{\mathrm{d}t}\frac{\partial}{\partial \dot q} T(q,\dot q) + u = 0$ and hence are equal to the forced Euler–Lagrange equations for L with forcing $f(q,\dot q,u) = \frac{\partial}{\partial q} v(q) = u$. Thus, the vector fields $X_{L^u} = X^u_{\mathrm{L}}$ coincide and therefore, $X^{u_{\mathrm{e}}}_{\mathrm{L}}(x_{\mathrm{e}}) \in T_{x_{\mathrm{e}}}(G \cdot x_{\mathrm{e}})$, i.e. $(x_{\mathrm{e}}, u_{\mathrm{e}})$ is a trim primitive as defined in Definition 3.6. □

Note that in Theorem 3.7 the condition that the controlled potential is G-invariant implicitly gives restrictions on v and thus on the control u. The forced Noether's Theorem 3.3 suggests candidates for trim primitives, namely all trajectories with such controls that act orthogonal to the group action. Indeed the following corollary states that this orthogonality condition is in fact necessary for the construction of trim primitives.

Corollary 3.8 *If $x_{\mathrm{e}} = (q_{\mathrm{e}}, v_{\mathrm{e}})$ with control u_{e} is a trim primitive of a Lagrangian system with symmetry group G and G-invariant controlled potential $V^{u_{\mathrm{e}}} = V(q) - v(q)$ with $\frac{\partial}{\partial q} v(q) = u_{\mathrm{e}}$, it necessarily holds that $u_{\mathrm{e}} \cdot \xi_Q(q_{\mathrm{e}}) = 0$, with $\cdot$ denoting the standard scalar product. Here, ξ_Q is the infinitesimal generator of $\xi \in \mathfrak{g}$ such that $(q,\dot q)(t) = \Phi^{TQ}(\exp(t\xi), (q_{\mathrm{e}}, v_{\mathrm{e}}))$, $u(t) \equiv u_{\mathrm{e}}$ is a solution of the forced Euler–Lagrange equations.*

Proof It follows from the G-invariance of L that the original V is G-invariant, because we assume G to act by isometries and the kinetic energy is given in terms of a metric. Then, from the G-invariance of $V^{u_{\mathrm{e}}}$, i.e. $V^{u_{\mathrm{e}}}(\Phi(g,q)) = V^{u_{\mathrm{e}}}(q)$, it can be deduced that

$$V\big(\Phi(g,q)\big) - v\big(\Phi(g,q)\big) = V(q) - v(q) \quad \Leftrightarrow \quad v\big(\Phi(g,q)\big) - v(q) = 0.$$

As g is a point in the one-parameter subgroup $\mathbb{R} \ni s \to \exp(s\xi) \in G$ generated by $\xi \in \mathfrak{g}$, we can replace g by $\exp(s\xi)$, set q to the trim primitive value x_{e} and then

differentiate with respect to s and evaluate at $s = 0$:

$$0 = \frac{\mathrm{d}}{\mathrm{d}s}\big(v\big(\Phi\big(\exp(s\xi), q_\mathrm{e}\big)\big) - v(q_\mathrm{e})\big)\Big|_{s=0}$$
$$= \frac{\partial}{\partial q} v\big(\Phi\big(\exp(s\xi), q_\mathrm{e}\big)\big) \cdot \frac{\mathrm{d}}{\mathrm{d}s}\Phi\big(\exp(s\xi), q_\mathrm{e}\big)\Big|_{s=0} = u_\mathrm{e} \cdot \xi_Q(q_\mathrm{e}). \qquad \square$$

Hence, we received a necessary condition on u_e to be admissible for a trim primitive that can be used to compute trim primitives in example systems.

Note that depending on the system under consideration, it is not guaranteed to identify all trim primitives by numerically finding the zeros of the gradient of the amended potential. However, restricting to only some of all existing trim primitives does not make the motion planning approach fail. However, it does in fact reduce the number of controllable states.

3.3 Invariant Manifolds in Natural Dynamics

In this section, we analyze the system's *natural dynamics*, i.e. the unforced case of e.g. a mechanical system. Nonlinear dynamical systems may exhibit complicated structures, e.g. local attractors or invariant manifolds (Guckenheimer and Holmes 1983) that separate the state space. These structures are not at all obvious up to a careful and systematic analysis. However, there may be motions of the unforced system that can be of great interest in control problems when searching for energy efficient solutions. Stable manifolds are introduced in a number of textbooks on dynamical systems (e.g. Guckenheimer and Holmes 1983; Katok and Hasselblatt 1995 among others or Abraham and Marsden 1987 for mechanical systems). The following definitions are basically taken from the latter with a slightly different notation at some points.

Consider a vector field X on a manifold with its corresponding flow F^t, e.g. a Lagrangian vector field X_L on the tangent bundle TQ with flow $F_\mathrm{L}^t : TQ \to TQ$. A *critical element* is either an *equilibrium*, i.e. a point $\bar{x} \in TQ$ such that $X_\mathrm{L}(\bar{x}) = 0$ and, hence, $F_\mathrm{L}^t(\bar{x}) = \bar{x}$ for all $t \in \mathbb{R}$, or a *closed orbit*, i.e. the orbit of a periodic point ($F_\mathrm{L}^t(\bar{x}) = F_\mathrm{L}^{t+\tau}(\bar{x})$ with $\tau > 0$ being the smallest value that satisfies this condition).

Given an equilibrium point $\bar{x}$, we are interested in the eigenvalues of $X'_\mathrm{L}(\bar{x})$, i.e. the linearization of X_L at $\bar{x}$, $X'_\mathrm{L}(\bar{x}) : T_{\bar{x}}(TQ) \to T_{\bar{x}}(TQ)$ defined by $X'_\mathrm{L}(\bar{x}) \cdot v = \frac{\mathrm{d}}{\mathrm{d}\lambda}(TF_\mathrm{L}^\lambda(\bar{x}) \cdot v)|_{\lambda=0}$. In coordinates, the matrix $X'_\mathrm{L}(\bar{x})$ is given by $(\frac{\partial X_\mathrm{L}^i}{\partial x^j})|_{x=\bar{x}}$. It is a well known stability criterion that a system is asymptotically (un)stable, if all eigenvalues have strictly negative (resp. positive) real parts. In the following, we will study the case where there are eigenvalues on both sides of the imaginary axis. A critical point is called *hyperbolic*, if none of the corresponding linearization eigenvalues has zero real part.

To investigate the dynamic behavior near closed orbits, the Poincaré map of a transversal section S is studied. A *transversal section* of X_L at a point x on the orbit is a submanifold $S \subset TQ$ of codimension one with $x \in S$ and for all $s \in S$, $X_\mathrm{L}(s)$ is not contained in $T_s S$. Then, roughly speaking, the *Poincaré map* of a closed orbit γ is a diffeomorphism Θ between neighborhoods of x in S that assigns to each

neighboring point $s \in S$ the point, where the orbit $F_{\mathrm{L}}^{\rho(s)}(s)$ intersects S again for the first time. Here, $\rho(s)$ is the corresponding return time. (For a detailed description we refer to Abraham and Marsden 1987 or another textbook on dynamical systems.) For a closed orbit γ of a vector field X_{L}, the *characteristic multipliers* of X_{L} at γ are the eigenvalues of $T_x\Theta$ for any Poincaré map Θ at any $x \in \gamma$. γ is called *hyperbolic*, if none of the characteristic multipliers has modulus one. Analogous to the stability criterion of Lyapunov for equilibria, a period orbit is asymptotically (un)stable, if the modulus of all characteristic multipliers is less (resp. greater) than one.

Theorem 3.9 (cf. Abraham and Marsden 1987) *If $\gamma \subset TQ$ is a critical element of X_{L}, there exist submanifolds of TQ, i.e. local stable ($W^{\mathrm{s}}_{\mathrm{loc}}$), center-stable ($W^{\mathrm{cs}}_{\mathrm{loc}}$), center ($W^{\mathrm{c}}_{\mathrm{loc}}$), center-unstable ($W^{\mathrm{cu}}_{\mathrm{loc}}$), and unstable ($W^{\mathrm{u}}_{\mathrm{loc}}$) manifolds, respectively, with the following properties*:

(i) *each submanifold is invariant under X_{L} and contains γ,*
(ii) *For $x \in \gamma$, $T_x(W^{\mathrm{s}}_{\mathrm{loc}})$ is the sum of the eigenspace in $T_x(TQ)$ of the characteristic multipliers of modulus <1 and the subspace $T_x\gamma$; $T_x(W^{\mathrm{cs}}_{\mathrm{loc}})$ (resp. $T_x(W^{\mathrm{c}}_{\mathrm{loc}})$, $T_x(W^{\mathrm{cu}}_{\mathrm{loc}})$, $T_x(W^{\mathrm{u}}_{\mathrm{loc}})$) is the sum of the eigenspace in $T_x(TQ)$ of the characteristic multipliers of modulus ≤ 1 (resp. $=1$, ≥ 1, >1) and the subspace $T_x\gamma$.*
(iii) *If $x \in W^{\mathrm{s}}_{\mathrm{loc}}$, then the ω-limit, given by $\omega(x) = \bigcap_{T=0}^{\infty} \overline{(\bigcup_{t \geq T} F_{\mathrm{L}}^t(x))}$ is equal to γ. If $x \in W^{\mathrm{u}}_{\mathrm{loc}}$, then the α-limit is γ, with $\alpha(x) = \bigcap_{T=0}^{-\infty} \overline{(\bigcup_{t \leq T} F_{\mathrm{L}}^t(x))}$.*
(iv) *$W^{\mathrm{s}}_{\mathrm{loc}}$ and $W^{\mathrm{u}}_{\mathrm{loc}}$ are locally unique.*

Thus, all points of the local stable manifold $W^{\mathrm{s}}_{\mathrm{loc}}$ tend to the critical element under the evolution. Conversely, the local unstable manifold $W^{\mathrm{u}}_{\mathrm{loc}}$ consists of all points in TQ which show this behavior if time runs backwards. The dynamics on the center manifold is subject to a further analysis (see e.g. Abraham and Marsden 1987 and the references therein) but out of the scope for this work.

Remark 3.10 In case of a critical point, i.e. an equilibrium $\gamma = \bar{x}$, the tangent space is trivial, $T_{\bar{x}}\gamma = \{0\}$ and therefore, $T_{\bar{x}}(W^{\mathrm{s}}_{\mathrm{loc}})$ equals the eigenspace in $T_{\bar{x}}(TQ)$ of the characteristic multipliers of modulus <1. Further, for $\gamma = \bar{x}$, the characteristic multipliers have to be interpreted as the eigenvalues of $T_{\bar{x}}F_{\mathrm{L}}^t$, i.e. $\mathrm{e}^{t\mu_1}, \ldots, \mathrm{e}^{t\mu_n}$ where $\mu_1, \ldots, \mu_n$ are the eigenvalues of $X'_{\mathrm{L}}(\bar{x})$ (also called characteristic exponents). In other words, the stable manifold $W^{\mathrm{s}}_{\mathrm{loc}}$, for example, is defined by the eigenvalues that lie in the strict left plane ($\mathfrak{Re}(\mu_i) < 0$). In contrast, for γ being a closed orbit, $T_{\bar{x}}\gamma$ is the subspace generated by $X(\bar{x})$ that is included in all of the submanifolds defined above.

Of special interest is the hyperbolic case, where there are no center eigenspaces. Then the nearby orbits of γ behave qualitatively like the linear case, i.e. for a hyperbolic critical point, the flow nearby looks like that of the linearization at γ.

Corollary 3.11 (Global stable manifold theorem of Smale, cf. Abraham and Marsden 1987) *If γ is hyperbolic, then the stable manifold, $W^{\mathrm{s}}(\gamma) = \{x \in TQ | \omega(x) \subset \gamma\}$ and the unstable manifold, $W^{\mathrm{u}}(\gamma) = \{x \in TQ | \alpha(x) \subset \gamma\}$ are immersed submanifolds.*

Also, $\gamma \subset W^{\mathrm{s}}(\gamma) \cap W^{\mathrm{u}}(\gamma)$ *and for* $x \in \gamma$, $T_x W^{\mathrm{s}}(\gamma)$ *and* $T_x W^{\mathrm{u}}(\gamma)$ *generate* $T_x(TQ)$. *If* n_s *is the number of characteristic multipliers of* γ *of modulus* <1, *and* n_u *the number of modulus* >1, *then the dimension of* $W^{\mathrm{s}}(\gamma)$ (*resp.* $W^{\mathrm{u}}(\gamma)$) *is* n_s (*resp.* n_u) *if* γ *is a critical point, or* $n_s + 1$ (*resp.* $n_u + 1$) *if* γ *is a closed orbit.*

That means, the local (un)stable manifolds defined in Theorem 3.9 can be uniquely expanded to global manifolds by applying the flow of the vector field.

So far, we have not covered all of the structure of critical points of Lagrangian systems. Since a regular Lagrangian system can be transformed into a Hamiltonian system by the Legendre transformation, the eigenvalue spectrum of a critical point can be characterized even further. It is a well known result (see e.g. Abraham and Marsden 1987) that the linearization of a Hamiltonian system is a linear Hamiltonian system and therefore, if μ is an eigenvalue of $X'_H(\bar{x})$, then so are $\bar{\mu}, -\mu, -\bar{\mu}$. Therefore, stable and unstable manifolds of a critical point always have the same dimension and the center manifold, if existent, is even dimensional. Additionally, for a Lagrangian that equals kinetic minus potential energy, solely the second-order partial derivatives of the potential, i.e. $\frac{\partial^2}{\partial q^2} V$ determine the spectral characteristics. From the Lagrange–Dirichlet stability criterion (see e.g. Abraham and Marsden 1987; Marsden 1993), it follows that the system is stable, if the matrix $\frac{\partial^2}{\partial q^2} V$ evaluated at the equilibrium is positive definite. Then the eigenvalues lie on the imaginary axis. Otherwise, the system is unstable, because there has to be at least one eigenvalue with positive real part giving rise to an unstable manifold.

For another extension of the preceding theory for critical points, let us assume that the strongest stable and unstable eigenvalues, i.e. $\mu^{\mathrm{ss}} := \min_{\mu \in \sigma} \mathfrak{Re}(\mu)$ and $\mu^{\mathrm{uu}} := \max_{\mu \in \sigma} \mathfrak{Re}(\mu)$ where σ denotes the eigenvalue spectrum of the linearization at the equilibrium $\bar{x}$, are unique and real. Then we define the *strong* (*un*)*stable manifolds* $W^{\mathrm{ss}}(\bar{x})$ and $W^{\mathrm{uu}}(\bar{x})$ as the submanifold of the (un)stable manifold that are tangent to the eigenspace corresponding to the strongest (un)stable eigenvalues μ^{ss} and μ^{uu} (see e.g. Osinga et al. 2004).

However, in most cases it is not possible to compute these global invariant manifolds analytically. For that reason, a number of numerical techniques for approximating (un)stable manifolds has been developed in the last decades (see Krauskopf et al. 2005 for an overview of existing approaches and a comprehensive comparison of the methods for the example of the Lorenz system). The different methods all share the idea to successively grow the (un)stable manifold from a local neighborhood of the equilibrium. Among these techniques is GAIO (*Global Analysis of Invariant Objects*), a set oriented method (cf. Dellnitz et al. 2001) that we use for our numerical examples.

As discussed in Sect. 1, invariant manifolds have been used in many applications in astrodynamics to generate low energy trajectories. In this setting, trajectories along invariant manifolds provide pieces of maneuver sequences that are solutions of optimal control problems in space mission design (cf. e.g. Koon et al. 2000 or Dellnitz et al. 2006, 2009 for approaches based on set oriented computations by GAIO).

4 Motion Planning Using Primitives

Now we go into more detail describing the computational aspects of motion planning with primitives. First it is shown how the identified dynamical structures can be used to generate motion primitives. The maneuver automaton is introduced to organize the primitives in a library. Secondly, trajectory generation and the computation of motion plans are presented.

4.1 Maneuver Automaton

A library of primitives constitutes a *maneuver automaton*, i.e. a finite-state machine with states and transitions corresponding to motion primitives (cf. Frazzoli et al. 2005). In our work, the states correspond not only to trim primitives, but also to (un)stable manifolds. The automaton's transitions between different states correspond to maneuvers, i.e. short motions satisfying the boundary conditions imposed by the initial and final states that they connect.

A library is constructed by selecting a discrete set of trim primitives and trajectories on (un)stable manifolds. Let Ξ denote the set of trims, chosen for instance by uniformly gridding a bounded subspace of the Lie algebra (see Definition 3.6), or alternatively by quantizing the space of internal (shape) variables and control input. For example, the elements of Ξ can be computed by the critical points of the controlled amended potential (cf. Sect. 3.2). It is sufficient to select and store only a trim's initial value $\alpha(0) := (x_\alpha(0), u_\alpha(0))$, because the orbit can be constructed by the flow, $\alpha : t \in [0, t_\mathrm{f}] \mapsto (\Phi^{TQ}(\exp(t\xi), x_\alpha(0)), u_\alpha)$ with $\xi \in \mathfrak{g}$ and a constant control $u_\alpha \equiv u_\alpha(0)$.

Analogously, a finite set $\mathcal{O}$ of orbits on (un)stable manifolds, $\mathcal{O} \ni O : t \in [0, t_\mathrm{f}] \mapsto F_\mathrm{L}(x_O, t)$ has to be defined with some initial value x_O on the manifold. For motion planning purposes it is advantageous to select orbits with fast dynamical transition. Such motions correspond to trajectories on the *strong* (un)stable manifolds, because these are the directions of the most contraction to (expansion from, respectively) a critical element. Such choices are reasonable since we are interested in energy minimal or time minimal solutions (cf. Sect. 2.1). Because the strong (un)stable manifolds are one-dimensional (assuming simple strong (un)stable eigenvalues as in Osinga et al. 2004), orbits $O \in \mathcal{O}$ can be computed by choosing a starting point x_O in the close neighborhood and evolving the uncontrolled flow for some finite time t_f; in forward time for unstable, and in backward time for stable manifolds, respectively.

A maneuver is then designed to connect pairs of trim primitives and pairs of orbits on manifolds as well as pairs of a trim primitive and a manifold orbit. A fully connected automaton graph would thus require $n_\mathrm{t}(n_\mathrm{t}-1)+n_\mathrm{o}(n_\mathrm{o}-1)+n_\mathrm{t}n_\mathrm{o}$ maneuvers, where $n_\mathrm{t} = \dim(\Xi)$ and $n_\mathrm{o} = \dim(\mathcal{O})$.

4.2 Maneuvers

We next describe the construction of maneuvers. Let the map $\varpi : X \to X\backslash G$ subtract out the invariant coordinates from a given state according to the system's symmetry

equivalence. Each maneuver is computed through nonlinear optimization of a trajectory whose start and end correspond to either a trim primitive or a manifold. This is defined through the following procedure:

$$\textit{Compute}: \quad t_\mathrm{f};\, x : [0, t_\mathrm{f}] \to X;\; u : [0, t_\mathrm{f}] \to U \tag{11}$$

$$\textit{minimizing}: \quad J(x, u, t_\mathrm{f}) = \int_0^{t_\mathrm{f}} \left(\lambda_1 \cdot 1 + \lambda_2 \cdot \left\|u(t)\right\|^2\right) \mathrm{d}t, \tag{12}$$

$$\textit{subject to}: \quad \text{dynamics equation (5) for all } t \in [0, t_\mathrm{f}] \tag{13}$$

and *one* of the following boundary conditions:

$$\text{from trim } x_\alpha \text{ to trim } x_\beta: \quad \varpi\left(x(0)\right) \in \varpi(x_\alpha), \varpi\left(x(t_\mathrm{f})\right) \in \varpi(x_\beta), \tag{14}$$

$$\text{from trim } x_\alpha \text{ to manifold } O_\beta: \quad \varpi\left(x(0)\right) \in \varpi(x_\alpha), \varpi\left(x(t_\mathrm{f})\right) \in \varpi(O_\beta), \tag{15}$$

$$\text{from manifold } O_\alpha \text{ to trim } x_\beta: \quad \varpi\left(x(0)\right) \in \varpi(O_\alpha), \varpi\left(x(t_\mathrm{f})\right) \in \varpi(x_\beta), \tag{16}$$

$$\text{from manifold } O_\alpha \text{ to manifold } O_\beta: \quad \varpi\left(x(0)\right) \in \varpi(O_\alpha), \varpi\left(x(t_\mathrm{f})\right) \in \varpi(O_\beta), \tag{17}$$

with $\lambda_1, \lambda_2 \in \mathbb{R}_0^+$ and where $\varpi(x_\alpha)$ should be understood as a pointwise evaluation. In essence, the optimization is performed by not enforcing a given final group displacement or by allowing a maneuver to start and end anywhere on the initial and final manifold orbits, respectively.

Definition 4.1 (Maneuvers) A *maneuver* is a solution pair $\pi := (x^*, u^*)$, $\pi : t \in [0, t_\mathrm{f}] \mapsto (q^*(t), \dot{q}^*(t), u^*(t))$ to (11)–(17) that connects two automaton states, i.e. trim primitives or (un)stable manifolds.

More generally, the boundary constraints can adapted based on the problem. For instance, using the identity instead of ϖ in (14)–(17), the points on the primitives are completely fixed (including the invariant coordinates). This is important, if one wants to control the group displacement of the maneuver (cf. Sect. 4.3). In addition, a boundary point on a manifold orbit can either be a fixed point on the orbit, or an analytic expression of the entire orbit (or an approximation of it, e.g. by splines) can be used as a boundary constraint. As another design parameter, the weighting $\lambda_{1,2}$ has to be chosen to prioritize one objective over the other. Naturally in most applications, energy efficiency is contradictory to time optimality, rendering a multiobjective optimal control problem. That means that different values of $\lambda_{1,2}$ correspond to different optimal compromises of the concurring objectives—the so called *Pareto optimal solution* (Ehrgott 2005) of the optimal control problem. The prioritization of objectives leads to a scalarization of the vector valued cost functional. If this cannot or is not desired to be done in advance, several optimal control maneuvers for the same boundary conditions, but different values of $\lambda_{1,2}$ can be computed and stored in the motion planning library.

In our applications, the optimizations were performed offline such that all maneuvers are organized and saved in a library which is loaded at run-time providing instant

look-up during planning. The continuous optimal control formulation was computationally solved through the discrete mechanics methodology DMOC (Ober-Blöbaum et al. 2011; Marsden and West 2001; Kobilarov 2008) which is particularly suitable for systems with nonlinear state spaces and symmetries.

The key property of motion primitives is that they can be concatenated to create more complex motion sequences. Following Frazzoli et al. (2005), a concatenation of two motion primitives $\pi_1 : t \in [0, t_{\mathrm{f},1}] \mapsto (x_1(t), u_1(t))$ and $\pi_2 : t \in [0, t_{\mathrm{f},2}] \mapsto (x_2(t), u_2(t))$ on the time interval $[0, t_{\mathrm{f},1} + t_{\mathrm{f},2}]$ is defined by

$$\pi_1\pi_2(t) := \begin{cases} (x_1(t), u_1(t)) & \text{if } t \le t_{\mathrm{f},1}, \\ (\Phi^{TQ}(g_{12}, x_2(t - t_{\mathrm{f},1})), u_2(t - t_{\mathrm{f},1})) & \text{otherwise,} \end{cases}$$

if there exists a group element g_{12} such that the second motion can be shifted compatibly, i.e. it holds $x_1(t_{\mathrm{f},1}) = \Phi^{TQ}(g_{12}, x_2(0))$. Furthermore, a trajectory π connecting two trims x_α and x_β by means of a motion along an (un)stable manifold orbit $O \in \mathcal{O}$ can be regarded as an *extended maneuver*.

Definition 4.2 (Extended Maneuvers) Let x_α, x_β $(\alpha \neq \beta)$ be trims and let $O \in \mathcal{O}$ be an (un)stable manifold orbit. Let π_1 be the maneuver of duration t_1 connecting x_α and O, and π_2 the maneuver connecting O and x_β. Define $\kappa : t \in [t_1, \tilde{t}] \mapsto (F_{\mathrm{L}}(x_1(t_1), t), 0)$, $\tilde{t} \ge t_1$ as that piece of the trajectory on O (with zero control) that starts at the final state of maneuver π_1 with duration $\tilde{t} - t_1$, s.t. $x_2(0) = F_{\mathrm{L}}(x_1(t), \tilde{t} - t_1)$. Then an extended maneuver π is defined as

$$\pi = \pi_1\kappa\pi_2.$$

Recall that the dynamical system is assumed to be autonomous, so time shifts are well defined. Controllability of the maneuver automaton is proved in Frazzoli et al. (2005) and still holds in the same sense for our motion planning approach applied to the trims and extended maneuvers.

4.3 Trajectory Generation

Consider the task of generating a trajectory from a given state $x_0 \in X$. It is typical to assume that this is either an equilibrium or periodic motion corresponding to a trim primitive. Denote the primitive by α_0 with initial state $x_{\alpha_0}(0)$. Then we have $x_0 = \Phi^{TQ}(g_0, x_{\alpha_0}(0))$ for some $g_0 \in G$. A trim primitive can be parametrized by its time duration, called the *coasting time* τ, leading to a family of trims, $\alpha(\tau) : t \in [0, \tau] \mapsto (\Phi^{TQ}(\exp(t\xi_\alpha, x_\alpha(0))), u_\alpha)$.

Consider a sequence of trim primitives $\alpha_0, \alpha_1, \ldots, \alpha_N$ with coasting times $\tau_0, \tau_1, \ldots, \tau_N$ and connecting maneuvers $\pi_0, \ldots, \pi_{N-1}$. These maneuvers can be either regular or extended. They form the trajectory ρ starting from x_0, defined by

$$\rho = \alpha_0(\tau_0)\pi_0\alpha_1(\tau_1)\pi_1 \cdots \alpha_N(\tau_{N-1})\pi_{N-1}\alpha_N(\tau_N). \tag{18}$$

The states along ρ are expressed, for $k \geq 0$, by

$$\rho(t) = \begin{cases} (\Phi^{TQ}(g_k \exp((t-t_k)\xi_{\alpha_k}), x_{\alpha_k}(0)), u_{\alpha_k}), & t \in [t_k, t_k + \tau_k], \\ (\Phi^{TQ}(g_k \exp(\tau_k \xi_{\alpha_k}), x_{\pi_k}(t')), u_{\pi_k}(t')), & t \in [t_k + \tau_k, t_{k+1}], \end{cases} \tag{19}$$

where $g_k = g_0 \prod_{i=0}^{k-1} \exp(\tau_i \xi_{\alpha_i}) g_{\pi_i}$, $t_k = \sum_{i=0}^{k-1} (\tau_i + |\pi_i|)$, with duration $|\pi_i|$ of maneuver π_i, and $t' = t - t_k - \tau_k$. The group elements $\exp(\tau_i \xi_{\alpha_i})$ are trim displacements, whereas g_{π_i} are the displacements of the maneuvers π_i. In addition, the total group displacement along ρ is

$$g_\rho = g_N \exp(\tau_N \xi_{\alpha_N}). \tag{20}$$

4.4 Computing Motion Plans

Next, consider the task of finding a sequence of primitives driving the system from its initial state x_0 to a given final state $x_\mathrm{f} \in \mathcal{X}_\mathrm{f}$. Let α_0 and α_f denote the given boundary trims with initial states $x_{\alpha_0}(0)$ and $x_{\alpha_\mathrm{f}}(0)$. Then we have $x_0 = \Phi^{TQ}(g_0, x_{\alpha_0}(0))$ and $x_\mathrm{f} = \Phi^{TQ}(g_\mathrm{f}, x_{\alpha_\mathrm{f}}(0))$ for some group elements $g_0, g_\mathrm{f} \in G$.

Computing a motion from x_0 to x_f amounts to finding a proper sequence of trim primitives $\alpha_0, \ldots, \alpha_N, \alpha_\mathrm{f}$, coasting times $\tau_0, \tau_1, \ldots, \tau_N, \tau_\mathrm{f}$, and connecting maneuvers $\pi_0, \ldots, \pi_N$ some of which include motions along (un)stable manifold orbits $O \in \mathcal{O}$. The sequence will form the trajectory ρ defined by

$$\rho = \alpha_0(\tau_0)\pi_0\alpha_1(\tau_1)\pi_1 \cdots \alpha_N(\tau_N)\pi_N\alpha_\mathrm{f}(\tau_\mathrm{f}). \tag{21}$$

The total group displacement along ρ is

$$g_\rho = \left[\prod_{i=0}^{N} \exp(\tau_i \xi_{\alpha_i}) g_{\pi_i}\right] \exp(\tau_\mathrm{f} \xi_{\alpha_\mathrm{f}}) \tag{22}$$

and computing a motion from x_0 to x_f amounts to finding a motion plan ρ such that

$$g_\rho = g_0^{-1} g_\mathrm{f}. \tag{23}$$

An optimal sequence of primitives and manifolds orbits should minimize the cost function $J(\rho)$. Although this is generally a complex combinatorial optimization with nonlinear constraints, it is much easier to solve than the original optimal control problem. The first reason is that the length of the sequence of required primitives is usually known in advance. For instance, in addition to the initial and final trim in general at least $\max(n-2, 0)$ additional (intermediate) trims are required to exactly satisfy any boundary conditions for an n-dimensional group G. In addition, in many cases the condition (23) can be solved analytically by computing the required trim coasting times using kinematic inversion.

Our implementation is based on a search tree (see Fig. 1) which expands all possible sequences of trims and manifold orbits and connecting maneuvers. The tree is grown in depth-first manner so that each trajectory contains $\max(n, 2)$ trim primitives. The search space is pruned using bounds on the optimal cost that is updated

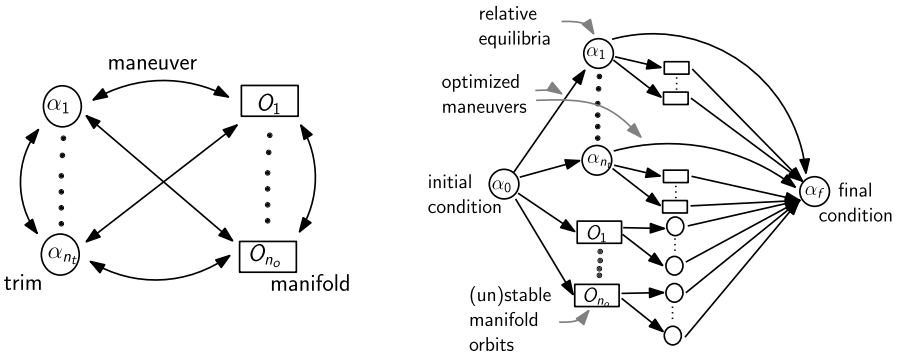

Fig. 1 *Left*: An automaton with states corresponding to relative equilibria and (un)stable manifolds and transitions corresponding to maneuvers. *Right*: An example of a search tree expanding paths of various sequences of primitives. This particular tree has three trim primitives and each trajectory must end at trim state α_f. The goal is to find a sequence and the coasting times along its relative equilibria so that the group displacement is satisfied and the total cost is minimized

Table 1 Combinations of primitives for $n = 1, 2, 3$

dim(G)	sequence	# of trims	# of maneuvers (depth)
1	$\alpha_0\pi_0\alpha_f$	2	1
	$\alpha_0\pi_0 O_1\pi_1\alpha_f$		2
2	$\alpha_0\pi_0\alpha_f$	2	1
	$\alpha_0\pi_0 O_1\pi_1\alpha_f$		2
3	$\alpha_0\pi_0\alpha_1\pi_1\alpha_f$,	3	2
	$\alpha_0\pi_0 O_1\pi_1\alpha_1\pi_2\alpha_f$		3
	$\alpha_0\pi_0\alpha_1\pi_2 O_1\pi_3\alpha_f$		3
	$\alpha_0\pi_0 O_1\pi_1\alpha_1\pi_2 O_2\pi_3\alpha_f$		4

during the algorithm operation. Thus, the number of primitives along trajectories in the tree varies from $2n - 1$ (when no manifolds are visited) to $4n - 3$ (when alternating between visiting trims and manifolds). For instance, for $n = 3$ the shortest sequence is $\alpha_0\pi_0\alpha_1\pi_1\alpha_f$ while the longest is $\alpha_0\pi_0 O_1\pi_1\alpha_1\pi_2 O_2\pi_3\alpha_f$. Table 1 lists the combinations of primitives up to $n = 3$.

Such sequences are automatically created by the tree-expansion algorithm for a given Lie group G. Note that we have assumed that all trims are non-equilibrium. Boundary conditions corresponding to equilibrium states (i.e. zero velocity) are handled by creating a sequence with an additional maneuver to or from a non-zero trim primitive.

By the construction of the maneuver automaton, the sequence ρ is a dynamically feasible solution for the optimal control problem from the initial state x_0 to the final state x_f. Thus, it can be used as a good initial guess for a post-optimization, e.g. performed by DMOC again. If the maneuver automaton is small, i.e. the gridding of trim and manifold state space is rough and the number of different connecting maneuvers

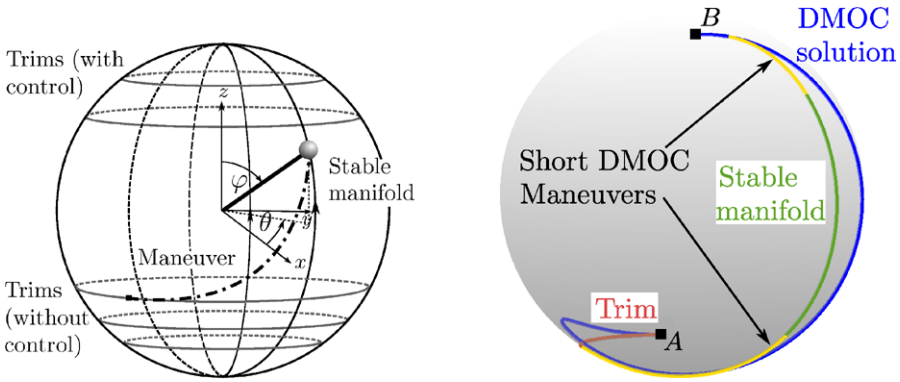

Fig. 2 *Left*: Model of the simple spherical pendulum with sketched motion primitives in configuration space: trims are purely horizontal motions ($\dot{\varphi} = 0$), whereas the (un)stable manifold are vertical motions ($\dot{\theta} = 0$). *Right*: Optimal sequence for a scenario from trim A to trim B consisting of the trims, two controlled maneuvers and a trajectory on the stable manifold in between. The *blue curve* is the solution of a DMOC optimization with the sequence as initial guess (Color figure online)

is small, a post-optimization is useful to smooth out the changes between controlled and uncontrolled pieces of the sequence trajectory. Furthermore, post-optimization is also required if the weighing of the (concurrent) objectives has to be updated or adjusted.

5 Numerical Examples

The simple spherical pendulum, i.e. a mass point moving in 3D constrained on a sphere, is a popular example to study symmetries of a mechanical system (see, among others Marsden 1993; Abraham and Marsden 1987; Bullo and Lewis 2004) and can be also used to demonstrate our motion planning approach (cf. Flaßkamp et al. 2010). From the application point of view, spherical pendula can be seen as idealizations of industrial robots, for example a double spherical pendulum is a simplified two-link manipulator. Therefore, optimal control of spherical pendula is of great importance.

5.1 The Spherical Pendulum

The pendulum consists of a point mass with mass m that is firmly connected by a massless rod of length r to the ground. Thus, the configuration space of this two degree of freedom system is a sphere. In coordinates, it can be described by a vertical angle, denoted by φ and a horizontal angle, denoted by θ (cf. Fig. 2).

Invariance and Symmetry The Lagrangian is given by $L(\varphi, \dot{\theta}, \dot{\varphi}) = K(\varphi, \dot{\theta}, \dot{\varphi}) - V(\varphi) = \frac{1}{2}mr^2(\dot{\varphi}^2 + \dot{\theta}^2 \sin^2(\varphi)) - mgr(\cos(\varphi) + 1)$. It can be easily seen that L is independent of θ, which is therefore called a *cyclic coordinate* (cf. e.g. Bloch 2003). Thus, it follows directly from $\frac{\partial L}{\partial \theta} = 0$ that the corresponding Euler–Lagrange equations simplify to $\frac{\partial L}{\partial \theta} = \text{const}$. In other words, the system is symmetric w.r.t. rotations

about the vertical axis and the symmetry group is $G = S^1$, acting by addition only in the horizontal coordinate. Therefore, the conserved quantity equals $p_\theta = \frac{\partial L}{\partial \dot{\theta}}$, that is, the momentum map $J = p_\theta = mr^2 \sin^2(\varphi)\dot{\theta}$. The Hamiltonian as the system's energy is given by $E(q, \dot{q}) = K(q, \dot{q}) + V(q)$. The amended potential is then given by $V_\mu(q) = V(q) + \frac{1}{2}\langle \mu, \mathbb{I}^{-1}\mu \rangle = mgr(\cos(\varphi) + 1) + \frac{1}{2}\mu^2(mr^2 \sin^2(\varphi))^{-1}$. Relative equilibria can be computed as critical points of V_μ and fulfill $\dot{\theta}^2 = -\frac{g}{r \cdot \cos(\varphi)}$, i.e. they are purely horizontal rotations ($\dot{\varphi} = 0$) in the lower hemisphere. A discrete set Ξ of uncontrolled trims (cf. Sect. 4.1) for $\varphi \in \{\frac{2}{3}\pi, \frac{3}{4}\pi, \frac{5}{6}\pi\}$ for example, can be defined by the rotational velocity, i.e. the Lie group elements $\Xi = \{\pm\sqrt{2\frac{g}{r}}, \pm\sqrt{\sqrt{2}\frac{g}{r}}, \pm\sqrt{\frac{2\sqrt{3}}{3}\frac{g}{r}}\}$. If we add control in φ-direction, the rotational velocity and the height of a trim can be chosen arbitrarily with $u_\varphi = -mgr \sin(\varphi) - mr^2 \sin(\varphi)\cos(\varphi)\dot{\theta}^2$.

(Un)stable Manifolds of the Upper Equilibrium The *planar pendulum* exhibits a hyperbolic equilibrium in the upper fixed point. This gives rise to one-dimensional stable and unstable manifolds; together they form the separatrix in the well known phase portrait of a simple pendulum. For purely vertical initial conditions ($\dot{\theta} = 0$), the spherical pendulum behaves like a planar pendulum. This, together with the horizontal symmetry, explains why the stable and unstable manifold of the upper equilibrium of the spherical pendulum are given by $W^{\mathrm{u,s}}(\bar{x}) = \{(q, \dot{q}) \in TQ \mid J(q, \dot{q}) = 0, E(q, \dot{q}) = V(\bar{x}) = 2mgr\} = \{(\theta, \varphi, \dot{\theta}, \dot{\varphi}) | \theta = \text{const.}, \dot{\theta} = 0, \dot{\varphi}^2 = 2\frac{g}{r}(1 - \cos(\varphi))\}$, i.e. the manifolds of the planar pendulum with an arbitrary, but fixed horizontal angle.

Motion Planning Trim primitives are uniform rotations in horizontal planes, whereas trajectories on the (un)stable manifolds are purely vertical motions. Choosing a discretization in both angles (plus a discretization of the rotational velocity for trim primitives in case of non-zero control) gives the motion primitives for the library (see Fig. 2 (left) for a sketch of the motion primitives). For numerical computations, all parameters are normalized to one. The connecting maneuvers are computed by DMOC. Here we allow forcing in both coordinate directions and search for solutions that minimize $J(x, u) = \int_0^{t_\mathrm{f}} (u_\theta(t)^2 + u_\varphi(t)^2)\,\mathrm{d}t$. As an exemplary scenario we choose a starting point A and a final point B on trims ($\varphi_A = \frac{13}{16}\pi$ uncontrolled, $\varphi_B = \frac{1}{8}\pi$ controlled s.t. $\dot{\theta} = -\pi$) and search for sequences with minimal control effort that connect these trims with a trajectory on the stable manifold to the upper equilibrium by maneuvers. The resulting trajectory (cf. Fig. 2 (right)) has the costs $J = 3.2211$ and the final time $t_\mathrm{f} = 4.3335$, which is the sum of the time spent on the trims, the fixed durations of the maneuvers and the time that the sequence stays on the manifold orbit. The sequence is then used as an initial guess for a post-optimization by DMOC that reduces the costs of the sequence to $J = 1.3821$. This is compared to optimal solutions of naive, direct optimizations with simple linearly interpolated initial guesses, i.e. we interpolate each coordinate between its initial and final point on an equidistant time grid. Such an initial guess can be constructed without any knowledge of the dynamical system, however, the resulting curve is by no means an admissible solution. It turns out that the information about the duration of the optimal trajectory that we obtain from the sequencing approach is important for finding energy efficient maneuvers: direct solutions for $t_\mathrm{f} = 2$ or $t_\mathrm{f} = 12$ have much higher costs

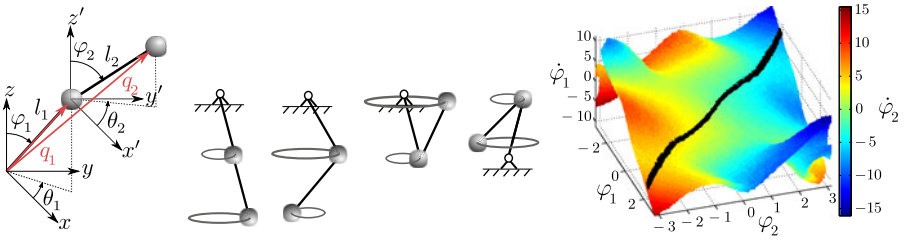

Fig. 3 *Left*: Model of the double spherical pendulum. *Middle*: Shape of the relative equilibria without control. Adding constant control in vertical direction also allows for trim primitives with both pendula pointing upwards and an arbitrary jointly rotational velocity (not shown). *Right*: Approximation of the stable manifold of the upper equilibrium and the strong stable manifold in black, computed by GAIO (Color figure online)

of $J = 6.3427$ and $J = 2.6084$. For the time t_f defined by the sequence, the direct solutions are similar in cost and qualitative behavior compared to the sequence. In more complicated systems, such as a double spherical pendulum, it is much harder to find any reasonable, admissible solution without choosing a sophisticated initial guess.

5.2 The Double Spherical Pendulum

In case of a double spherical pendulum, a mixture of analytical and computational methods have to be applied to compute the motion primitives. In the following, we will present candidates for a motion planning library and afterwards, show numerical results for specific optimal control scenarios.

Euler–Lagrange Equations The configuration space of two 3D pendula, idealized as mass points m_1 and m_2 on massless rods, is $Q = S^2_{l_1} \times S^2_{l_2}$, where $S^2_{l_{1,2}}$ denotes the two dimensional sphere of radius $l_{1,2}$. As a minimal set of coordinates, we choose horizontal and vertical angles ($q = (\theta_1, \theta_2, \varphi_1, \varphi_2)$), such that the mass points positions are given by (cf. Fig. 3)

$$q_1 = \begin{pmatrix} x_1 \\ y_1 \\ z_1 \end{pmatrix} = \begin{pmatrix} l_1 \cos(\theta_1) \sin(\varphi_1) \\ l_1 \sin(\theta_1) \sin(\varphi_1) \\ l_1 \cos(\varphi_1) \end{pmatrix},$$

$$q_2 = \begin{pmatrix} x_2 \\ y_2 \\ z_2 \end{pmatrix} = \begin{pmatrix} x_1 \\ y_1 \\ z_1 \end{pmatrix} + \begin{pmatrix} l_2 \cos(\theta_2) \sin(\varphi_2) \\ l_2 \sin(\theta_2) \sin(\varphi_2) \\ l_2 \cos(\varphi_2) \end{pmatrix}.$$

The Lagrangian as the difference of kinetic and potential energy can be written as $L(q(t), \dot{q}(t)) = K(q(t), \dot{q}(t)) - V(q(t))$, where $V(q(t)) = (m_1 + m_2) g l_1 (\cos(\varphi_1) + 1) + m_2 g l_2 (\cos(\varphi_2) + 1)$, and $K(q(t), \dot{q}(t)) = \frac{1}{2} \dot{q}^T(t) M(q(t)) \dot{q}(t)$ with the symmetric mass matrix $M = (m_{ij})$ with $m_{11} = (m_1 + m_2) l_1^2 \cdot \sin^2(\varphi_1)$, $m_{12} = m_2 l_1 l_2 \cdot \cos(\theta_1 - \theta_2) \cdot \sin(\varphi_1) \sin(\varphi_2)$, $m_{13} = 0$, $m_{14} = -m_2 l_1 l_2 \sin(\theta_1 - \theta_2) \cdot \sin(\varphi_1) \cos(\varphi_2)$, $m_{22} = m_2 l_2^2 \sin^2(\varphi_2)$, $m_{23} = m_2 l_1 l_2 \cdot \sin(\theta_1 - \theta_2) \cdot \cos(\varphi_1) \sin(\varphi_2)$, $m_{24} = 0$, $m_{33} = (m_1 + m_2) l_1^2$, $m_{34} = m_2 l_1 l_2 ((\cos(\theta_1 - \theta_2) \cdot \cos(\varphi_1) \cos(\varphi_2)) \sin(\varphi_1) \sin(\varphi_2))$, $m_{44} = m_2 l_2^2$.

Hence, the Euler–Lagrange equations for the double spherical pendulum without forcing are

$$\frac{\mathrm{d}}{\mathrm{d}t}\frac{\partial L}{\partial \dot{\varphi}_{1,2}} - \frac{\partial L}{\partial \varphi_{1,2}} = 0, \qquad \frac{\mathrm{d}}{\mathrm{d}t}\frac{\partial L}{\partial \dot{\theta}_{1,2}} - \frac{\partial L}{\partial \theta_{1,2}} = 0. \tag{24}$$

Symmetry and Reduction The symmetry group is $G = S_1$, acting by rotation of both pendula about the z-axis: $\Phi : G \times Q \to Q$, $\Phi(g, (\theta_1, \theta_2, \varphi_1, \varphi_2)) = (g + \theta_1, g + \theta_2, \varphi_1, \varphi_2)$ with tangent lift to TQ by $\Phi_g^{TQ}(q, v) = (\Phi(g, q), \dot{\theta}_1, \dot{\theta}_2, \dot{\varphi}_1, \dot{\varphi}_2)$. Then the infinitesimal generator can be determined to be $\xi_Q(q) = (\xi, \xi, 0, 0)^{\mathrm{T}}$ with $\xi \in \mathbb{R}$. Hence, the conserved quantity is the total angular momentum about the z-axis

$$J(q, v) = \frac{\partial L}{\partial \dot{\theta}_1} + \frac{\partial L}{\partial \dot{\theta}_2}, \tag{25}$$

and the locked inertia tensor (cf. Sect. 3.2) equals

$$\begin{aligned}\mathbb{I}\big(q(t)\big) = {} & (m_1 + m_2) l_1^2 \sin^2(\varphi_1) + m_2 l_2^2 \sin^2(\varphi_2) \\ & + 2 m_2 l_1 l_2 \cos(\theta_1 - \theta_2) \cdot \sin(\varphi_1) \sin(\varphi_2).\end{aligned}$$

The mechanical connection $\alpha : TQ \to \mathfrak{g}$ can be easily computed by $\alpha(q, v) = \mathbb{I}^{-1}(q) \cdot J(q, v)$, assigning to each (q, v) the angular velocity of the locked system (cf. Marsden and Scheurle 1993). The amended potential can be computed by

$$V_\mu\big(q(t)\big) = V\big(q(t)\big) + \frac{\mu^2}{2\mathbb{I}(q)}.$$

Trims Trims of the uncontrolled system, i.e. relative equilibria, are classified in (Marsden and Scheurle 1993) in an elegant way by introducing two shape defining parameters and then computing the critical points of the amended potential (cf. the Lagrangian reduction in Sect. 3.2). Besides the four true equilibria (each pendulum either pointing straight upwards or downwards), all relative equilibria are given by a one-parameter curve and they look similar to one of the four sketched types in Fig. 3 (middle). According to Definition 3.6, non-zero constant control values are allowed, if they do not influence the conservation of the angular momentum J (cf. (25)). Hence, we add forcing in φ_1- and φ_2-direction in (24). This leads to a controlled potential and we can therefore solve $\frac{\partial}{\partial q} V_\mu = -u$ for constant $u = (0, 0, u_{\varphi_1}, u_{\varphi_2})^{\mathrm{T}}$ as proposed by Theorem 3.7. This additionally admits trims with both pendula pointing upwards as well as arbitrary rotating velocities in all shapes.

Manifolds For this example, we are interested in the (un)stable manifold of the upper equilibrium, i.e. both pendula pointing upwards ($\bar{x} = (\bar{q}, \dot{\bar{q}}) = 0_{8\times 1}$). In this point, the system's energy equals $E_{\bar{x}} := V(\bar{q})$ while the angular momentum is zero. Hence the manifolds are part of the set $\{x \in TQ \mid E(x) = E_{\bar{x}}, J(x) = 0\}$. This includes in particular the motion on (un)stable manifolds of a planar double pendulum, to which we have restricted our computations so far. Since the manifolds are two dimensional, we still have to choose concrete trajectories that are stored in the motion planning

library. Here we use the strong (un)stable manifolds (cf. Sect. 4.1). In Fig. 3 (right) the black line corresponds to the approximation of the strong stable manifold in the stable manifold of the upper equilibrium, which has been computed with GAIO (cf. Sect. 3.3).

Numerical Results for Motion Planning Scenarios As mentioned before, we use the optimal control method DMOC (cf. Sect. 2.3) to compute connecting maneuvers between trims and orbits on manifolds. For numerical computations, we choose the following parameter values: $m_1 = m_2 = 1$ kg, $l_1 = l_2 = 1$ m, and $g = 9.81 \frac{\mathrm{m}}{\mathrm{s}^2}$. The nonlinear optimization problem is solved by an SQP method (cf. Sect. 2.1) of NAG[1] (*Numerical Algorithms Group*). To improve the accuracy of the derivatives that have to be provided, the implementation of the DMOC method has been combined with ADOL-C[2] (*Automatic Differentiation by OverLoading in C++*), an automatic differentiation technique, in Ober-Blöbaum and Walther (2010). For the connecting maneuvers, we allow an arbitrary boundary point on the specific trims (cf. (14)–(17)), i.e. the point is fixed except for the horizontal coordinates, which have to fulfill $\theta_1 = \theta_2$ for an arbitrary angle θ_1. Since the double spherical pendulum is modeled in minimal coordinates that are not globally valid, we are faced with singularities in our numerical computations. If one of the pendulum's vertical angle equals 0 or π (or multiplicities of that), the horizontal angle becomes meaningless. The NAG algorithm is able to perform the optimization for our scenarios. Nevertheless, to overcome this problem in principle, a global system description by e.g. differential algebraic models could be used in future work.

The motion planning is performed for the following scenario: the starting point is chosen to lie on an uncontrolled trim ($\varphi_1 = 2.4087$, $\varphi_2 = 2.2532$), where the double pendulum is outstretched. The final point is the upper equilibrium, i.e. both pendula pointing upwards. We consider the fully actuated system ($u = (u_{\theta_1}, u_{\theta_2}, u_{\varphi_1}, u_{\varphi_2})^{\mathrm{T}}$) and choose the control effort as the cost functional, i.e.

$$J\big(x(t), u(t)\big) = \int_0^{t_\mathrm{f}} u(t)^2 \,\mathrm{d}t \quad \text{with } u(t) \in \mathbb{R}^4.$$

According to the defined scenario, a sequence of depth 2 (cf. the definition of a search tree in Sect. 4.4) is searched for, consisting of a maneuver from the trim to the orbit of the strong stable manifold of the upper equilibrium and then a second, very short maneuver to bridge the gap from the orbit's endpoint to the equilibrium itself. Figure 4 shows a resulting sequence with duration $t_\mathrm{f} = 3.28$ and costs $J = 548.76$. The durations of the maneuvers have been fixed in advance, such that the entire duration depends on how long the sequence stays on the manifold orbit. The dashed lines refer to the results of a post-optimization performed by DMOC, which reduces the costs to $J = 296.51$. In comparison, when DMOC is directly applied to the problem with a simple, linearly interpolated initial guess, the retained optimal solution has much higher costs of $J = 5.85 \cdot 10^3$.

[1] www.nag.co.uk.

[2] https://projects.coin-or.org/ADOL-C.

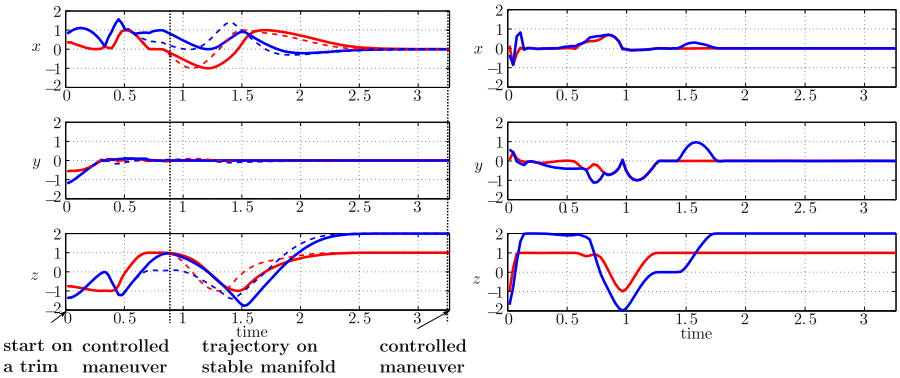

Fig. 4 *Left*: Sequence for an example scenario, presented in Cartesian coordinates of both pendula (*solid lines*; inner pendulum *red*, outer pendulum *blue*) and resulting optimal trajectory for a post-optimization with DMOC (*dashed lines*). *Right*: A maneuver resulting from an optimization by DMOC with simple initial guess (Color figure online)

In this scenario, we considered sequences involving only one manifold and therefore restricted to the stable manifold of the upper equilibrium. However, it might be possible that a sequence of higher depth including other manifolds as well would even lead to further improvement. This has to be studied in future work.

6 Conclusion and Outlook

This work proposes a motion planning strategy based on motion primitives encoding inherent dynamical system properties. We extend the approach of Frazzoli et al. (2005) by including motion primitives on (un)stable manifolds of critical elements of the uncontrolled dynamics. Such primitives are useful for finding energy efficient solutions, experimentally confirmed by the numerical results for our example optimal control scenarios. We study the motion primitives induced by symmetries in more detail, focusing on mechanical systems. Trim primitives for arbitrary mechanical systems are identified using Noether's theorem on conserved angular momenta through a symmetry reduction process. In addition to trim primitives and orbits on (un)stable manifolds, connecting maneuvers are computed by the optimal control method DMOC and stored in the motion planning library. The maneuver automaton of Frazzoli et al. (2005) is extended to include orbits on manifolds and finally we develop a tree search algorithm in this new automaton for motion planning. The application of the approach to the optimal control of a double spherical pendulum clearly shows that optimization using initial guesses, obtained by exploiting the key structural properties of the system, results improved solutions (w.r.t. to cost) compared to standard initialization.

Future work will apply this optimal control policy to more complex systems such as multi-body systems with holonomic (Leyendecker et al. 2009) or nonholonomic constraints (Kobilarov et al. 2010). For example, the structural properties of a rigid body pendulum that are revealed in Chaturvedi et al. (2011) could be used for optimal

control scenarios as well. In higher dimensional systems it will be more challenging to identify symmetries, i.e. Lie groups and admissible controls for trim primitives. If the computation of (un)stable manifolds gets numerically too expensive, invariant objects in a reduced system (e.g. obtained by Lagrangian reduction) could be considered. Alternatively, one could restrict oneself to the one-dimensional strong (un)stable manifolds.

Studying hybrid Lagrangian systems is another natural extension. A control sequence resulting from a motion planning procedure is already hybrid in the sense that different types of control trajectory are concatenated. Hybrid dynamics can also occur if different Lagrangian are valid in different regions of state space or because of impacts, i.e. instantaneous jumps in the states. Symmetry and reduction of hybrid Lagrangian systems has been already studied in e.g. Ames and Sastry (2006). Thus, it is desirable and conceptually possible to extend the motion planning approach to symmetric hybrid systems. If the motion planning library is designed to include many admissible sequences, our tree search can be augmented with a more efficient sampling strategy. A possible approach is to employ adaptive sampling used in the context of randomized motion planning (Kobilarov 2011).

Thinking further ahead, optimal control problems of complex dynamical systems will typically include not only one or two, but several, competing objectives. Additionally, a real world motion planning problem will include several boundary constraints, e.g. given by different operation points that have to be reached one after the other. These subproblems as well as the prioritized objective may change during an operation. For scenarios like this, a motion planning library that has been generated offline in advance seems appropriate for an online optimization.

Acknowledgements Jerry Marsden has been a great inspiration to us to work on this topic. We thank him for fruitful discussions and collaborations during the last years. This contribution was partly developed and published in the course of the Collaborative Research Centre 614 "Self-Optimizing Concepts and Structures in Mechanical Engineering" funded by the German Research Foundation (DFG) under grant number SFB 614.

M. Kobilarov was supported by the Keck Institute for Space Studies, Caltech.

References

Abraham, R., Marsden, J.E.: Foundations of Mechanics. Addison-Wesley, Redwood City (1987)

Ames, A.D., Sastry, S.: Hybrid Routhian reduction of Lagrangian hybrid systems. In: American Control Conference, 2006, June 2006. 6 pp.

Betts, J.T.: Survey of numerical methods for trajectory optimization. AIAA J. Guid. Control Dyn. **21**(2), 193–207 (1998)

Binder, T., Blank, L., Bock, H.G., Bulirsch, R., Dahmen, W., Diehl, M., Kronseder, T., Marquardt, W., Schlöder, J.P., von Stryk, O.: Introduction to model based optimization of chemical processes on moving horizons. In: Grötschel, M., Krumke, S.O., Rambau, J. (eds.) Online Optimization of Large Scale Systems: State of the Art, pp. 295–340. Springer, Berlin (2001)

Bloch, A.M.: Nonholonomic Mechanics and Control. Springer, Berlin (2003)

Bloch, A.M., Leonard, N.E., Marsden, J.E.: Controlled Lagrangians and the stabilization of mechanical systems. I. The first matching theorem. IEEE Trans. Autom. Control **45**(12), 2253–2270 (2000)

Bullo, F., Lewis, A.D.: Geometric Control of Mechanical Systems. Texts in Applied Mathematics, vol. 49. Springer, New York (2004)

Bullo, F., Lewis, A.: Reduction, linearization, and stability of relative equilibria for mechanical systems on Riemannian manifolds. Acta Appl. Math. **99**, 53–95 (2007)

Chaturvedi, N., Lee, T., Leok, M., McClamroch, N.: Nonlinear dynamics of the 3D pendulum. J. Nonlinear Sci. **21**, 3–32 (2011)
Choset, H., Lynch, K.M., Hutchinson, S., Kantor, G.A., Burgard, W., Kavraki, L.E., Thrun, S.: Principles of Robot Motion: Theory, Algorithms, and Implementations. MIT Press, Cambridge (2005)
Christensen, G.S., El-Hawary, E., Soliman, S.A.: Optimal Control Applications in Electric Power Systems. Mathematical Concepts and Methods in Science and Engineering, vol. 35. Plenum, New York (1987)
Conley, C.: Low energy transit orbits in the restricted three-body problem. SIAM J. Appl. Math. **16**, 732–746 (1968)
Dellnitz, M., Froyland, G., Junge, O.: The algorithms behind GAIO—set oriented numerical methods for dynamical systems. In: Fiedler, B. (ed.) Ergodic Theory, Analysis, and Efficient Simulation of Dynamical Systems, pp. 145–174. Springer, Berlin (2001)
Dellnitz, M., Junge, O., Post, M., Thiere, B.: On target for Venus—set oriented computation of energy efficient low thrust trajectories. Celest. Mech. Dyn. Astron. **95**, 357–370 (2006)
Dellnitz, M., Ober-Blöbaum, S., Post, M., Schütze, O., Thiere, B.: A multi-objective approach to the design of low thrust space trajectories using optimal control. Celest. Mech. Dyn. Astron. **105**, 33–59 (2009). doi:10.1007/s10569-009-9229-y
Ehrgott, M.: Multicriteria Optimization, 2nd edn. Springer, Berlin (2005)
Flaßkamp, K., Ober-Blöbaum, S.: Energy efficient control for mechanical systems based on inherent dynamical structures. In: American Control Conference (ACC), June 2012, Montréal, Canada, pp. 2609–2614 (2012)
Flaßkamp, K., Ober-Blöbaum, S., Kobilarov, M.: Solving optimal control problems by using inherent dynamical properties. PAMM **10**(1), 577–578 (2010)
Frazzoli, E., Dahleh, M.A., Feron, E.: Maneuver-based motion planning for nonlinear systems with symmetries. IEEE Trans. Robot. **21**(6), 1077–1091 (2005)
Froyland, G., Padberg, K.: Almost-invariant sets and invariant manifolds—connecting probabilistic and geometric descriptions of coherent structures in flows. Physica D **238**(16), 1507–1523 (2009)
Gerdts, M.: Solving mixed-integer optimal control problems by branch & bound: a case study from automobile test-driving with gear shift. Optim. Control Appl. Methods **26**(1), 1–18 (2005)
Gill, P.E., Jay, L.O., Leonard, M.W., Petzold, L.R., Sharma, V.: An SQP method for the optimal control of large-scale dynamical systems. J. Comput. Appl. Math. **120**, 197–213 (2000)
Gómez, G., Koon, W.S., Lo, M.W., Marsden, J.E., Masdemont, J., Ross, S.D.: Connecting orbits and invariant manifolds in the spatial three-body problem. Nonlinearity **17**, 1571–1606 (2004)
Griewank, A., Walther, A.: Evaluating Derivatives: Principles and Techniques of Algorithmic Differentiation, 2nd edn. SIAM, Philadelphia (2008)
Guckenheimer, J., Holmes, P.: Nonlinear Oscillations, Dynamical Systems, and Bifurcations of Vector Fields. Applied Mathematical Sciences, vol. 42. Springer, Berlin (1983)
Haller, G.: Distinguished material surfaces and coherent structures in 3d fluid flows. Physica D **149**, 248–277 (2001)
Haller, G., Yuan, G.: Lagrangian coherent structures and mixing in two-dimensional turbulence. Physica D **147**, 352–370 (2000)
Katok, A., Hasselblatt, B.: Introduction to the Modern Theory of Dynamical Systems. Encyclopedia of Mathematics and Its Applications. Cambridge University Press, Cambridge (1995)
Kobilarov, M.: Discrete geometric motion control of autonomous vehicles. PhD thesis, University of Southern California, USA (2008)
Kobilarov, M.: Cross-entropy randomized motion planning. In: Proceedings of Robotics: Science and Systems, Los Angeles, CA, USA, June 2011
Kobilarov, M., Marsden, J.E.: Discrete geometric optimal control on Lie groups. IEEE Trans. Robot. **27**(4), 641–655 (2011)
Kobilarov, M., Marsden, J.E., Sukhatme, G.S.: Geometric discretization of nonholonomic systems with symmetries. Discrete Contin. Dyn. Syst., Ser. S **3**(1), 61–84 (2010)
Koon, W.S., Lo, M.W., Marsden, J.E., Ross, S.D.: Shoot the Moon. Spacefl. Mech. **105**(2), 1017–1030 (2000)
Koon, W.S., Lo, M.W., Marsden, J.E., Ross, S.D.: Low energy transfer to the Moon. Celest. Mech. Dyn. Astron. **81**(1–2), 63–73 (2001)
Krauskopf, B., Osinga, H.M., Doedel, E.J., Henderson, M.E., Guckenheimer, J., Vladimirsky, A., Dellnitz, M., Junge, O.: A survey of methods for computing (un)stable manifolds of vector fields. Int. J. Bifurc. Chaos Appl. Sci. Eng. **15**(3), 763–791 (2005)
LaValle, S.M.: Planning Algorithms. Cambridge University Press, Cambridge (2006)

Leyendecker, S., Ober-Blöbaum, S., Marsden, J.E., Ortiz, M.: Discrete mechanics and optimal control for constrained systems. In: Optimal Control, Applications and Methods, 2009
Marsden, J.E.: Lectures on Mechanics. London Mathematical Society Lecture Note Series, vol. 174. Cambridge University Press, Cambridge (1993)
Marsden, J.E.: Geometric Mechanics, Stability, and Control, pp. 265–291. Springer, New York (1994)
Marsden, J.E., Ratiu, T.S.: Introduction to Mechanics and Symmetry, 2nd edn. Text in Applied Mathematics, vol. 17. Springer, Berlin (1999)
Marsden, J.E., Scheurle, J.: Lagrangian reduction and the double spherical pendulum. Z. Angew. Math. Phys. **44** (1993)
Marsden, J.E., West, M.: Discrete mechanics and variational integrators. Acta Numer. **10**, 357–514 (2001)
Marsden, J.E., Patrick, G.W., Shkoller, S.: Multisymplectic geometry, variational integrators, and nonlinear PDEs. Commun. Math. Phys. **199**, 351–395 (1998)
Marsden, J.E., Ratiu, T.S., Scheurle, J.: Reduction theory and the Lagrange–Routh equations. J. Math. Phys. **41**, 3379–3429 (2000)
McGehee, R.: Some homoclinic orbits for the restricted three-body problem. PhD thesis, University of Wisconsin (1969)
Naldi, R., Marconi, L.: Optimal transition maneuvers for a class of V/STOL aircraft. Automatica **47**(5), 870–879 (2011)
Neumaier, A.: Complete search in continuous global optimization and constraint satisfaction. Acta Numer. **13**, 271–369 (2004)
Ober-Blöbaum, S., Walther, A.: Computation of derivatives for structure preserving optimal control using automatic differentiation. PAMM **10**(1), 585–586 (2010)
Ober-Blöbaum, S., Junge, O., Marsden, J.E.: Discrete mechanics and optimal control: an analysis. Control Optim. Calc. Var. **17**(2), 322–352 (2011)
Osinga, H.M., Rokni Lamooki, G.R., Townley, S.: Numerical approximations of strong (un)stable manifolds. Dyn. Syst. **19**(3), 195–215 (2004)
Roberts, M., Wulff, C., Lamb, J.S.W.: Hamiltonian systems near relative equilibria. J. Differ. Equ. **179**(2), 562–604 (2002)
Serban, R., Koon, W.S., Lo, M.W., Marsden, J.E., Petzold, L.R., Ross, S.D., Wilson, R.S.: Halo orbit mission correction maneuvers using optimal control. Automatica **38**, 571–583 (2002)
Simo, J.C., Lewis, D., Marsden, J.E.: Stability of relative equilibria. Part I: the reduced energy-momentum method. Arch. Ration. Mech. Anal. **115**, 15–59 (1991)
Sussmann, H.J., Willems, J.C.: 300 years of optimal control: from the Brachystochrone to the maximum principle. IEEE Control Syst. **17**(3), 32–44 (1997)
Wulff, C., Schilder, F.: Numerical bifurcation of Hamiltonian relative periodic orbits. SIAM J. Appl. Dyn. Syst. **8**(3), 931–966 (2009)
Zhigljavsky, A., Zilinskas, A.: Stochastic Global Optimization. Springer Optimization and Its Applications. Springer, Berlin (2008)